Received: 8 November 2022 | Revised: 18 October 2023 | Accepted: 14 November 2023

IET Generation, Transmission & Distribution

DOI: 10.1049/gtd2.13062

The Institution of Engineering and Technology WILEY

ORIGINAL RESEARCH

A robust optimization approach for resiliency improvement in power distribution system

Reza Abshirini | **Mojtaba Najafi** | **Naghi Moaddabi Pirkolachahi**

Department of Electrical Engineering, Bushehr Branch, Islamic Azad University, Bushehr, Iran

Correspondence
Mojtaba Najafi, Department of Electrical Engineering, Bushehr Branch, Islamic Azad University, Bushehr, Iran.
Email: abshirinir@yahoo.com, mojtaba.najafi@iau.ac.ir, nimamoaddabi@aut.ac.ir

Abstract

The occurrence of natural disasters has led to an alarming increase in power interruptions, with severe impacts. Compounding this problem is the uncertain nature of data, which presents significant challenges in enhancing the resiliency of power distribution systems following such events. To tackle these issues, this paper introduces a robust optimization approach for improving the resiliency of power distribution systems. The approach encompasses crew teams for switching actions as part of the restoration process, along with demand response programs and mobile generators (MGs). By simultaneously leveraging these elements and considering the uncertainty associated with electrical load and electrical price, the resiliency of the system is enhanced. The objective function is trilevel, comprising minimum, maximum, and minimum functions. At the first level, the approach minimizes the cost of commitment of combined heat and power plants (CHPs) by taking into account the location of MGs and the reconfiguration structure in power distribution systems. The second level aims to identify the worst-case scenario for the uncertainty variables. Finally, the third level focuses on minimizing the total operation cost under the worst-case scenario using demand response programs. The proposed algorithm is implemented on an IEEE 33-bus test distribution system, with four different cases investigated.

1 | INTRODUCTION

Over the past few years, the occurrence of natural disasters has led to an increase in power interruptions, causing significant impacts [1]. The resulting catastrophic outcomes in society and the economy have highlighted the urgent need to improve the resilience of power systems [2]. Among the various components of the power infrastructure, power distribution networks have suffered extensive damage during these events, leaving many customers without power for extended periods. This necessitates the development of effective and swift reactions as a crucial requirement for enhancing the resiliency of power distribution systems [3]. Traditional restoration methods have proven inadequate for expeditiously restoring power to affected customers in such scenarios, prompting distribution system operators to seek improved approaches [4]. In recent times, microgrids have gained widespread adoption as a solution to enhance the reliability of power distribution systems and meet customer expectations [5–7]. Furthermore, microgrids have emerged as a promising strategy for bolstering the resiliency of distribution systems [8, 9]. Reference [10] proposes an outage management hierarchical structure that leverages multiple microgrids within distribution systems. Additionally, reference [11] introduces an optimization recovery model that involves allocating distributed generations and utilizing resilient microgrids to restore power to critical customers.

Mobile generators (MGs) play a crucial role in expediting the recovery process of interrupted electrical loads within power distribution systems [4]. These generators are especially practical when the distribution network becomes disconnected from the upstream network, a common occurrence during natural disasters [12]. Reference [12] presents a two-stage optimization approach for the placement of MGs, encompassing pre-allocation and real-time placement while considering their charging ability. Building upon this, reference [13] introduces

an innovative approach that adapts the utilization of multiple MGs to enhance the restoration process of important loads in distribution grids. Furthermore, reference [14] proposes a resiliency approach that focuses on recovering critical loads by strategically allocating and scheduling MGs, considering network reconfiguration. Additionally, reference [15] presents a comprehensive framework aimed at boosting resiliency through the combined utilization of MGs, grid reconfiguration, and repair crew teams to efficiently restore critical demand following an outage. Moreover, reference [16] optimizes the time required for repair crew teams to arrive at faulted zones and effectively schedules MGs to ensure the swift recovery of important loads.

The resiliency improvement of power distribution grids is contingent upon various data, some of which involve uncertainties. These uncertainties in the data can significantly impact the optimization process. Reference [4] introduces a robust optimization approach to enhance the resiliency of power distribution systems. The approach consists of two distinct phases. In the first phase, the optimization focuses on determining the optimal locations for MGs. Subsequently, in the second phase, the MGs are dispatched, and distribution grid reconfiguration is simultaneously implemented, taking into consideration the uncertainties inherent in the system data. However, it is important to note that the approach assumes a predetermined dataset about the systems, which may not always reflect realistic conditions. Additionally, reference [17] proposes a stochastic scheme for post-event actions in power distribution systems. This scheme incorporates network reconfiguration and leverages the utilization of MGs to enhance resiliency. Notably, the formulation accounts for uncertainties in data such as load demands and the duration required for MG utilization.

A new methodology is proposed in reference [18] to handle the uncertainties arising from the condition of switches and asynchronous data during the procedure of distribution system reconfiguration. However, it should be noted that this methodology does not account for mobile energy generation, which restricts the flexibility of the model. In contrast, reference [19] presents a robust optimization approach aimed at enhancing the resiliency of power distribution systems by incorporating MGs while considering the uncertainty associated with post-event information. Furthermore, in reference [20], the stochastic nature of power loads, branches, and routes is taken into account by employing multiple scenarios generated through Monte Carlo simulation. Nevertheless, the effectiveness of scenario-based algorithms is hindered by the challenge of obtaining sufficient historical data from natural disasters. To overcome this limitation, reference [21] introduces a set-based robust optimization approach that considers the rare range of uncertain data.

Reference [22] introduces a multi-objective restoration scheme designed to enhance the resilience of an energy distribution network. The primary objective of the scheme is to reduce load shedding throughout the restoration procedure, while the secondary objective is to minimize restoration cost, which may conflict with the first goal. To ensure the necessary flexibility in distribution network restoration, the scheme incorporates demand response programs, distributed energy resources (DERs), and microgrid development. The demand response programs encompass transferable, curtailable, and shiftable loads, while the DERs in the proposed model encompass various components such as generators, wind-based and photovoltaic (PV)-based units, as well as energy storage systems. Additionally, in [23], a hybrid stochastic-robust optimization (HSRO) method is employed to determine the optimal scheduling for a microgrid under both regular and resilient operating modes. The robust optimization technique is used to account for the influence of upstream grid pricing uncertainty on the optimal scheduling of microgrids. Moreover, stochastic optimization is employed to predict other significant uncertainties including wind power, PV power, and active/reactive electrical loads by generating a range of plausible scenarios.

In reference [24], a post-event restoration model is proposed to enhance the resilience of distribution systems by incorporating DERs. This model considers critical loads and interruptible loads as part of a demand response program, focusing on improving the resilience of distribution networks following human resource (HR) events. Furthermore, reference [25] introduces a model for microgrid creation that takes into account constraints related to voltage and power loss during operation, as well as the feasibility of power balancing. The model leverages mixed-integer linear programming (MILP) to assist in solving precise power flow equations and optimize the configuration and operation of the microgrid.

In reference [26], a chance-constrained optimum distribution network partitioning approach is proposed to identify the most suitable candidates for microgrid creation in the aftermath of HR events. The method aims to maximize the resilience of the distribution network by considering probabilistic constraints and selecting optimal locations for microgrid implementation. Additionally, reference [27] introduces a bi-level optimization model based on the master-slave technique (MST) to enhance the resilience of the distribution system following natural catastrophes, taking into account the accessibility of fast-charging stations. The lower level of the model calculates the dynamic charging demand of the in-service stations, considering the limitations of the transportation network. At the top level, the model establishes the island borders to maximize the recovered loads within the distribution system.

In reference [28], an MILP model is described, focusing on the recovery of critical loads during extreme events through microgrid formation and the optimal utilization of DERs. Additionally, [29] presents a single-objective model that aims to build microgrids using electric vehicles and direct load control, specifically targeting the restoration of key loads. The suggested approach in this study significantly improves computational efficiency by reducing the number of binary and continuous variables involved. Moreover, reference [30] offers a unique planning technique for distribution system planners to enhance the resilience of distribution networks when facing catastrophes. This technique formulates the problem as a two-stage stochastic programming model, addressing both emergency and typical conditions. In the initial stage, decisions are made regarding line hardening, distributed generation deployment, mobile emergency generator allocation, and tie

switch placement. In the second stage, the model minimizes the operation costs associated with forced load shedding, DG power production, and purchasing distribution system planner power from the upstream network, aiming to achieve a techno-economic compromise between investment costs and improved operation/resilience benefits across both planning and operation scales.

Reference [31] suggests a brand-new, three-stage stochastic planning model that addresses both the emergency reaction and planning phases of resilient distribution systems. In the initial stage, the model makes decisions regarding line hardening and DER installations, aiming to maximize the resilience of the distribution system. Moving to the second stage, the model utilizes provided scenarios to incorporate line outage uncertainty and form preliminary microgrids using a master-slave control approach. Non-anticipative limitations are also introduced to ensure that microgrid formation decisions account for line damage uncertainty. Finally, once the load demand is known, a demand-side management program is employed to minimize the cost of load shedding in each temporary microgrid. In a related study, reference [32] presents an innovative three-step stochastic planning model specifically for the allocation of distributed generation in resilient distribution systems. This model encompasses the planning stage, the preventative reaction stage, and the emergency response stage.

Table 1 provides a concise summary of the classification of previous resilience studies in power distribution systems. The table encompasses various aspects, including formulation, uncertainty considerations, objective functions, thermal load analysis, robust optimization techniques, and operational strategies. Notably, none of the articles discussed in the previous research consider a comprehensive joint scheme that incorporates both price and load model uncertainty, along with four distinct operational strategies: reconfiguration, utilization of DERs, implementation of demand response programs, and the use of MGs. There is a research gap in the integration of a thermal mathematical model into a robust optimization problem with a polyhedric uncertainty set, specifically using a mixed-integer linear programming (MILP) formulation. This formulation should effectively incorporate four operational strategies to enhance the resiliency of power distribution systems. Additionally, limited attention has been given to the economic aspects and the application of demand response programs for resiliency improvement in prior studies. To address these gaps, this paper presents a formulated robust optimization approach to enhance the resiliency of power distribution systems. The proposed approach considers uncertain variables related to both electrical loads and electrical prices. It further integrates crew teams for switching actions during the restoration process, deploys demand response programs, and leverages the use of both MGs and fixed DERs to enhance system resilience. The objective function of the proposed approach is tri-level, comprising minimum, maximum, and minimum functions. The first level minimizes the cost of commitment of combined heat and power (CHP) units while considering the location of MGs and the reconfiguration structure of power distribution systems. The second level seeks to identify the

TABLE 1 Survey of former resilience studies.

		Uncertainty		Objective function					Operational strategies				
Reference	Formulation	Price	Load	Load restoration	Operation cost	Thermal load	Robust optimization	Reconfiguration	Fixed distributed energy resources	Demand response program	Mobile generators
[22]	MILP		✓	✓	✓			✓	✓	✓	
[23]	MILP	✓	✓	✓	✓		✓		✓	✓	
[24]	MILP				✓			✓		✓	
[25]	MINLP			✓				✓			
[26]	MILP			✓				✓			
[27]	MILP			✓				✓	✓	✓	
[28]	MILP		✓	✓				✓	✓	✓	
[29]	MILP		✓		✓			✓		✓	
[30]	MILP		✓					✓	✓		✓
[31]	MILP		✓		✓			✓	✓	✓	
[32]	MILP		✓	✓	✓			✓			✓
This Study	MILP	✓	✓	✓	✓	✓	✓	✓	✓	✓	✓

worst-case scenario in terms of uncertainty variables. Finally, the third level minimizes the total operation cost under the worst-case scenario of stochastic data, utilizing demand response programs.

Regards, the main contributions of this manuscript are as below:

- An adaptable robust optimization methodology with a polyhedric uncertainty set is presented for enhancing resiliency in power distribution systems. The methodology takes into account both electrical load and electrical price uncertainties. We introduce a budget of uncertainty index to adjust the trade-off between robustness and total cost, providing a novel approach to handle uncertainty.
- The paper investigates the effect of four post-event actions on system resiliency simultaneously. These actions include switching actions performed by crew teams during the restoration process, the application of demand response programs, and the utilization of MGs and fixed DERs. By examining these actions collectively, we offer insights into their combined effectiveness in improving system resilience.
- The study examines the impact of the number of crew teams for switching actions and the number of MGs on the robust resiliency approach. It allows the distribution system operator to select the appropriate number of these tools based on their specific operational requirements, providing flexibility and customization options.
- Unlike prior studies, our approach considers the thermal model in the resiliency problem. By integrating the thermal model, it is accounted for the thermal constraints and dynamics of the power distribution system, enabling more accurate and realistic analysis.

The rest of the article is arranged as follows: the robust resiliency model is introduced in the Section 2. The solution methodology is proposed in the Section 3. The case study is presented in Section 4. Moreover, the proposed robust resiliency formulation is implemented on an IEEE 33 bus distribution system and the obtained results are published and analysed in Section 5. Finally, conclusions are reported in the Section 6.

2 | PROBLEM FORMULATION

This manuscript proposes a robust optimization approach polyhedric uncertainty set for improving resiliency in power distribution systems. the polyhedral uncertainty set is a type of uncertainty set used in robust optimization, defined by a finite number of linear inequalities. It allows for the optimization of systems under uncertain conditions and provides a more accurate representation of uncertainty, including correlated uncertainties. Here, the polyhedric uncertainty set in robust optimization is handled with using Bertsimas method. The Bertsimas method is a widely used robust optimization technique that aims to find optimal solutions considering various scenarios and uncertainty. It has applications in finance, engineering, and operations research. The approach involves accepting suboptimal solutions for nominal data values to ensure feasibility and near-optimality under changing data conditions. The level of conservatism in the robust solutions can be adjusted using probabilistic bounds of constraint violations. The general structure of the robust optimization approach for resiliency enhancement is shown in Figure 1. The proposed robust formulation for resiliency enhancement is presented as a linear optimization problem, with the specific details of the problem formulation introduced in the upcoming sub-sections.

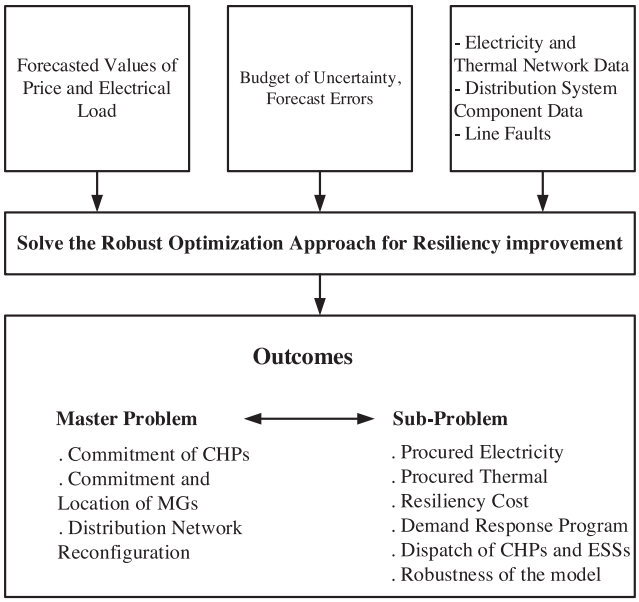

FIGURE 1 General structure of the robust optimization approach for resiliency enhancement.

2.1 | Uncertainty modelling

This approach involves determining specific intervals to address variable uncertainties. Equation (1) introduces an uncertain set Ø for stochastic variables, enabling the extraction of variable values from this set. Furthermore, a parameter known as the "budget of uncertainty" Γ, defined in Equation (1), is used to manage the deviation of uncertain variables from their predicted values. This parameter plays a crucial role in governing the robust resiliency model.

$$\emptyset = \left\{ \begin{array}{c} \sum_{t\in\Omega^T} \left| \frac{P_{it}^{ED} - \bar{P}_{it}^{ED}}{\hat{P}_{it}^{ED}} \right| \le \Gamma_P, \bar{P}_{it}^{ED} - \hat{P}_{it}^{ED} \le P_{it}^{ED} \le \bar{P}_{it}^{ED} + \hat{P}_{it}^{ED} \\ \sum_{t\in\Omega^T} \left| \frac{\lambda_t - \overline{\lambda_t}}{\hat{\lambda}_t} \right| \le \Gamma_\lambda, \overline{\lambda_t} - \hat{\lambda}_t \le \lambda_t \le \overline{\lambda_t} + \hat{\lambda}_t \end{array} \right\}$$

$$\forall t \in \Omega^T, i \in \Omega^{Bus}. \quad (1)$$

This paper delves into the analysis of stochastic variables, namely the electrical loads ($\bar{P}_{it}^{ED}$) and electrical price ($\overline{\lambda_t}$). Equation (1) introduces the nominal (forecasted) values of these variables, denoted as $\bar{P}_{it}^{ED}$ and $\overline{\lambda_t}$, along with the corresponding

errors, $\hat{P}_{it}^{ED}$ and $\hat{\lambda}_t$. The errors are expressed as a percentage ($E\%$) of the forecasted values. To address the optimization formulation's extreme points on the polyhedric vertices defined in Equation (1), a set of binary variables (v) is introduced. The transformation of continuous variables to binary variables (v^{t+}, v^{t-}) is explained in Equations (2)–(7), where Equation (2) specifically illustrates how the binary variables represent the electrical loads (P_{it}^{ED}) in relation to the nominal value, error, and binary variables themselves. Constraints in Equations (3) and (4) ensure that the binary variables satisfy specific conditions, limiting their value range. Similarly, Equations (5)–(7) outline the transformation of electrical prices (λ_t) into binary variables, accompanied by the corresponding constraints. Overall, the utilization of binary variables allows for the conversion of continuous variables into binary form, enabling the linearization of the dual function in the solution approach.

$$P_{it}^{ED} = \bar{P}_{it}^{ED} + \hat{P}_{it}^{ED} \times v_{i,P}^{t+} - \hat{P}_{it}^{ED} \times v_{i,P}^{t-} \; \forall t \in \Omega^T, i \in \Omega^{Bus}. \tag{2}$$

$$v_{i,P}^{t+} + v_{i,P}^{t-} \leq 1 \; \forall t \in \Omega^T, i \in \Omega^{Bus}. \tag{3}$$

$$\sum_{t \in \Omega^T} \left(v_{i,P}^{t+} + v_{i,P}^{t-} \right) \leq \Gamma_P \; \forall i \in \Omega^{Bus}. \tag{4}$$

$$\lambda_t = \overline{\lambda_t} + \hat{\lambda}_t \times v_{i,\lambda}^{t+} - \hat{\lambda}_t \times v_{i,\lambda}^{t-} \; \forall t \in \Omega^T. \tag{5}$$

$$v_{i,\lambda}^{t+} + v_{i,\lambda}^{t-} \leq 1 \; \forall t \in \Omega^T, i \in \Omega^{Bus}. \tag{6}$$

$$\sum_{t \in \Omega^T} \left(v_{i,\lambda}^{t+} + v_{i,\lambda}^{t-} \right) \leq \Gamma_\lambda \tag{7}$$

2.2 | Objective function

The robust resiliency optimization problem' objective function as Equation (8) revolves around minimizing the total cost of power distribution grids before and after a disastrous incident. This cost encompasses various components, such as total operation costs, total customer interruption costs, and total demand response costs. The objective function specifically focuses on the worst-case scenario, aiming to minimize costs under the highest level of uncertainty within the given uncertainty set [33]. Adjusting the degree of robustness is possible by manipulating the budget of uncertainty, which influences the total cost compared to a deterministic model. Notably, the objective function places significant emphasis on total customer interruption costs and incorporates the resiliency objective of maximizing the sum of restored curtailment loads alongside operation and demand response costs. The objective function is structured as a tri-level formulation, incorporating minimum, maximum, and minimum functions. The first level utilizes a minimum function to minimize the cost of commitment for CHPs, accounting for start-up and shutdown costs while considering the location of MGs and the reconfiguration structure within power distribution systems. The second level employs a maximum function to determine the worst-case scenario within the uncertainty set ∅. Finally, the third level minimizes the total operation cost of CHPs, MGs, and energy storage systems (ESSs), in addition to considering total customer interruption costs, total gas costs, total emission costs, total sold and purchased electricity costs, and total demand response costs under the worst-case scenario of stochastic data.

$$\begin{aligned} OF = \min_{u_{ig}^{chp}, sui_{it}^{CHP}, sdi_{it}^{CHP}, \delta_{i,it}, \beta_{li}, \varphi_{li}, u_t^{MG}, z_{it}^{\zeta}, z_{it}^{d}, ex_t^{in}, ex_t^{out}} \left(\sum_{t \in \Omega^T} \sum_{i \in \Omega^{Bus}} \left(c^{sp} \times sui_{it}^{CHP} + \right. \right. \\ c^{sd} \times sdi_{it}^{CHP} \Big) + \max_{\varphi} \min_{P_t^{buy}, P_t^{sell}, P_{it}^{DR}, P_{it}^{TDR}, P_{it}^{ESS}, P_{it}^{shed}, P_{it}^{Tshed}} \left[\sum_{t \in \Omega^T} \sum_{i \in \Omega^{Bus}} \left(CP_{it}^{CHP} + \right. \right. \\ CP_{it}^{MG} \Big) + \sum_{t \in \Omega^T} \sum_{i \in \Omega^{Bus}} \left(\lambda_t^{gas} \times v_{it}^{gas} \right) + \sum_{i \in \Omega^{Bus}} \sum_{t \in \Omega^T} \left(\rho_i^{EP} \times P_{it}^{shed} + \rho_i^{TP} \times \right. \\ P_{it}^{Tshed} \Big) + \sum_{t \in \Omega^T} c_t^{em} \times Em_t + \sum_{t \in \Omega^T} \left(\lambda_t \times P_t^{buy} - \lambda_t \times P_t^{sell} \right) + \\ \sum_{t \in \Omega^T} \sum_{i \in \Omega^{Bus}} \left(\omega^{DR} \times \lambda_t \times P_{it}^{DR} + \omega^{TDR} \times \lambda_t \times P_{it}^{TDR} \right) + \\ \left. \left. \left. \sum_{t \in \Omega^T} \sum_{i \in \Omega^{Bus}} \lambda_t \times P_{it}^{ESS} \right] \right) \end{aligned} \tag{8}$$

2.3 | Constraints

Equations (9)–(56) encompass the constraints of the robust optimization resiliency approach. These equations introduce the dual variable n, y_n^{it}, associated with bus i in the distribution system at time t. The total energy cost (TEC) is presented in Equation (9) and comprises the total cost of the grid (TC^{Grid}), total cost of natural gas (TC^{Gas}), total demand response cost (TC^{DR}), total cost of CHPs (TC^{CHP}), and total cost of ESSs (TC^{ESS}). For clarity, Equations (10)–(14) specify the individual expressions for TC^{Grid}, TC^{Gas}, TC^{DR}, TC^{CHP} and TC^{ESS}. The total customer interruption costs ($TCIC$) and total emission cost ($TCEM$) are addressed in Equations (15) and (16), respectively. Moreover, Equation (18) calculates the gas volume consumed by the distribution system at time t, represented as v_{it}^{gas}. Regarding the CHPs, Equation (19) considers the startup and shutdown status, taking into account the situation of CHPs at times $t-1$ and t.

$$TEC = TC^{Grid} + TC^{Gas} + TC^{DR} + TC^{CHP} + TC^{ESS} \tag{9}$$

$$TC^{Grid} = \sum_{t \in \Omega^T} \left(\lambda_t^{buy} \times P_t^{buy} - \lambda_t^{sell} \times P_t^{sell} \right) \tag{10}$$

$$TC^{Gas} = \sum_{t \in \Omega^T} \sum_{i \in \Omega^{Bus}} \left(\lambda_t^{gas} \times v_{it}^{gas} \right) \tag{11}$$

$$TC^{DR} = \sum_{t \in \Omega^T} \sum_{i \in \Omega^{Bus}} \left(\lambda_{it}^{DR} \times P_{it}^{DR} + \lambda_{it}^{TDR} \times P_{it}^{TDR} \right) \tag{12}$$

$$TC^{CHP} = \sum_{t \in \Omega^T} \sum_{i \in \Omega^{Bus}} \left(c^{sp} \times sui_{it}^{CHP} + c^{sd} \times sdi_{it}^{CHP} + CP_{it}^{CHP} \right) \tag{13}$$

$$TC^{ESS} = \sum_{t\in\Omega^T}\sum_{i\in\Omega^{Bus}} \lambda_{it}^{EP} \times P_{it}^{ESS} \tag{14}$$

$$TCIC = \sum_{i\in\Omega^{Bus}}\sum_{t\in\Omega^T} \left(\rho_i^{EP} \times P_{it}^{shed} + \rho_i^{TP} \times P_{it}^{Tshed}\right) \tag{15}$$

$$TCEM = \sum_{t\in\Omega^T} c_t^{em} \times Em_t \tag{16}$$

$$Em_t = em^{grid} \times P_t^{buy} + \sum_{i\in\Omega^{Bus}} \left(em^{chp} \times P_{it}^{CHP} + em^{axb} \times H_{it}^{AXB}\right) \ \forall t \in \Omega^T. \tag{17}$$

$$v_{it}^{gas} = G_{ref}^{CHP} \times \frac{P_{it}^{CHP}}{\eta_e} + G_{ref}^{AXB} \times \frac{H_{it}^{AXB}}{\eta_{axb}} \ \forall t \in \Omega^T, i \in \Omega^{Bus}. \tag{18}$$

$$sui_{it}^{CHP} - sdi_{it}^{CHP} = u_{it}^{chp} - u_{i(t-1)}^{chp} \ \forall t \in \Omega^T, \ i \in \Omega^{Bus}. \tag{19}$$

To ensure the proper operation of the power distribution grid, a radial structure must be maintained, which is achieved by satisfying constraints (20)–(22) [35]. Constraint (20) states that when a switch in a line is closed, either δ_{ijt} or δ_{jit} must be equal to one [35]. In this context, δ_{ijt} represents a binary variable that equals one if bus j serves as the parent of bus i at time t. Constraint (21) guarantees that each node, except for the root node, has a maximum of one parent. Additionally, constraint (22) specifies that the root node has no parents. To maintain system stability, the maximum change in the condition of each switch is limited to one within the planning horizon, as represented by Equation (23). This means that any changes in the status of lines (open or closed) must adhere to the conditions outlined in Equations (24) and (25), respectively. Furthermore, the number of switching actions is restricted by the number of crew groups, ensuring efficient management of resources, as described in Equation (26). Lastly, the number of MGs is limited based on the constraints defined in Equation (27).

$$\delta_{ijt} + \delta_{jit} = \beta_{lt} \ \forall t \in \Omega^T, i, j \in \Omega^{Bus}, \ l \in \Omega^i. \tag{20}$$

$$\sum_{j\in\Omega^i} \delta_{ijt} \le 1 \ \forall t \in \Omega^T, i \in \Omega^{Bus}. \tag{21}$$

$$\delta_{1jt} = 0 \ \forall t \in \Omega^T, j \in \Omega^{Bus}. \tag{22}$$

$$\sum_{t\in\Omega^T} \vartheta_{lt} \le 1 \ \forall l \in \Omega^l. \tag{23}$$

$$-\vartheta_{lt} \le \beta_{lt} - \beta_{l(t-1)} \le \vartheta_{lt} \ \forall t \in \Omega^T, l \in \Omega^l. \tag{24}$$

$$\vartheta_{lt} \le \beta_{lt} + \beta_{l(t-1)} \le 2 - \vartheta_{lt} \ \forall t \in \Omega^T, l \in \Omega^l. \tag{25}$$

$$\sum_{t\in\Omega^T} \vartheta_{lt} \le NCrew \ \forall, l \in \Omega^{maneuver}. \tag{26}$$

$$\sum_{i\in\Omega^{Bus}} u_i^{MG} \le NMG \tag{27}$$

Equations (28)–(31) provide the linearized operation costs for CHPs, while Equations (32)–(35) outline the linearized DistFlow equations [15]. The equilibrium of active power and reactive power at each node in the distribution system is achieved through Equations (32) and (33), respectively. The voltage magnitude at each bus in the distribution system is calculated using Equations (34) and (35). Notably, the big-M technique is employed to independently determine the voltages of two connected buses when the line is in an open condition. Equation (36) establishes the relationship between the power flow in a line, the switch condition (open or closed), and the line power capacity. To ensure the stability of the system, the voltage magnitude at each bus must fall within a specified standard range during normal operation, as described in Equation (37). Thermal flow balance is maintained through Equation (38). Additionally, the operational constraints of MGs, CHPs, and ESSs are taken into account, as detailed in Equations (39)–(49) respectively. The values of active power bought from and sold to the main network are restricted within the distribution system, as mentioned in Equations (50)–(54) respectively. Furthermore, Equations (55) and (56) limit the participation of electrical and thermal demands in the demand response program.

$$CP_{it}^{CHP} = A_i \times u_{it}^{chp} + \sum_{ll=1}^{NL_i} \alpha_{lli} \times \gamma_{llit} \ \forall t \in \Omega^T, i \in \Omega^{Bus}. \tag{28}$$

$$A_i = a_i + b_i \times \underline{P}_i^{CHP} + c_i \times (\underline{P}_i^{CHP})^2 \forall i \in \Omega^{Bus}. \tag{29}$$

$$P_{it}^{CHP} = \sum_{ll=1}^{NL_i} \gamma_{llit} + \underline{P}_i^{CHP} \times u_{it}^{chp} \ : y_1^{it} \forall t \in \Omega^T, i \in \Omega^{Bus}. \tag{30}$$

$$0 \le \gamma_{llit} \le PL_{lli} - PL_{(ll-1)i} \ : y_2^{llit} \ \forall t \in \Omega^T, i \in \Omega^{Bus}, ll \in \Omega^{NL}. \tag{31}$$

$$P_{it}^{ED} - P_{it}^{CHP} - P_{it}^{ESS} - P_{it}^{W} - P_{it}^{PV} - P_{it}^{DR} - P_{it}^{shed} - P_{it}^{MG} + P_t^{sell} - P_t^{buy} + \sum_{l\in\Omega^i} P_{lt}^{f} = 0 \ : y_3^{it} \quad \forall t \in \Omega^T, \ i \in \Omega^{Bus}. \tag{32}$$

$$Q_{it}^{ED} - Q_{it}^{CHP} - Q_{it}^{DR} - Q_{it}^{shed} - Q_{it}^{MG} + Q_t^{sell} - Q_t^{buy} + \sum_{l\in\Omega^i} Q_{lt}^{f} = 0 \ : y_4^{it} \quad \forall t \in \Omega^T, \ i \in \Omega^{Bus}. \tag{33}$$

$$V_{jt} - V_{it} + \frac{r_l \times P_{lt}^{f} + x_l \times Q_{lt}^{f}}{V_1} \ge (\beta_{lt} - 1) \times M \ : y_5^{ijlt} \ \forall t \in \Omega^T, \ i, j \in \Omega^{Bus}, l \in \Omega^i. \tag{34}$$

$$V_{jt} - V_{it} + \frac{r_l \times P_{lt}^{f} + x_l \times Q_{lt}^{f}}{V_1} \leq (1 - \beta_{lt}) \times M \ : y_6^{ijlt} \ \forall t \in \Omega^T,\ i, j \in \Omega^{Bus}, l \in \Omega^i. \tag{35}$$

$$-\beta_{lt} \times cap_l \leq P_{lt}^{f} \leq \beta_{lt} \times cap_l \ : y_7^{lt}, y_8^{lt} \ \forall t \in \Omega^T,\ l \in \Omega^i. \tag{36}$$

$$\underline{V} \leq V_{it} \leq \overline{V} \ : y_9^{it}, y_{10}^{it} t \in \Omega^T, i \in \Omega^{Bus}. \tag{37}$$

$$P_{it}^{TD} - P_{it}^{CHP} \times \left(\frac{\eta_{th}}{\eta_e}\right) - H_{it}^{AXB} - P_{it}^{TDR} - P_{it}^{Tshed} = 0 \ : y_{11}^{it} \ \forall t \in \Omega^T,\ i \in \Omega^{Bus}. \tag{38}$$

$$0 \leq P_{it}^{MG} \leq \bar{P}_i^{MG} \times u_i^{MG} \ : y_{12}^{it} \ \forall t \in \Omega^T,\ i \in \Omega^{Bus}. \tag{39}$$

$$0 \leq Q_{it}^{MG} \leq \bar{Q}_i^{MG} \times u_i^{MG} \ : y_{13}^{it} \ \forall t \in \Omega^T,\ i \in \Omega^{Bus}. \tag{40}$$

$$\underline{P^{CHP}} \times u_{it}^{chp} \leq P_{it}^{CHP} \leq \overline{P^{CHP}} \times u_{it}^{chp} \ : y_{14}^{it}, y_{15}^{it} \ \forall t \in \Omega^T,\ i \in \Omega^{Bus}. \tag{41}$$

$$\underline{Q^{CHP}} \times u_{it}^{chp} \leq Q_{it}^{CHP} \leq \overline{Q^{CHP}} \times u_{it}^{chp} \ : y_{16}^{it}, y_{17}^{it} \ \forall t \in \Omega^T,\ i \in \Omega^{Bus}. \tag{42}$$

$$P_{it}^{CHP} - P_{i(t-1)}^{CHP} \leq \left(2 - u_{i(t-1)}^{chp} - u_{it}^{chp}\right) \times \underline{P^{CHP}} + \left(1 + u_{i(t-1)}^{chp} - u_{it}^{chp}\right) \times RU^{CHP} \ : y_{18}^{it} \quad \forall t \in \Omega^T,\ i \in \Omega^{Bus}. \tag{43}$$

$$P_{i(t-1)}^{CHP} - P_{it}^{CHP} \leq \left(2 - u_{i(t-1)}^{chp} - u_{it}^{chp}\right) \times \underline{P^{CHP}} + \left(1 - u_{i(t-1)}^{chp} + u_{it}^{chp}\right) \times RD^{CHP} \ : y_{19}^{it} \quad \forall t \in \Omega^T,\ i \in \Omega^{Bus}. \tag{44}$$

$$P_{it}^{ESS} = E^{ESS} \times \eta_{\frac{ch}{dch}} \times \left(SOC_{i(t-1)} - SOC_{it}\right) \ : y_{20}^{it} \ \forall i \in \Omega^{Bus},\ t \in \Omega^T. \tag{45}$$

$$P_{it}^{ESS} \geq z_{it}^{c} \times \underline{P^{BI}} - z_{it}^{d} \times \overline{P^{BO}} \ : y_{21}^{it} \ \forall i \in \Omega^{Bus},\ t \in \Omega^T. \tag{46}$$

$$P_{it}^{ESS} \leq z_{it}^{c} \times \overline{P^{BI}} - z_{it}^{d} \times \underline{P^{BO}} \ : y_{22}^{it} \ \forall i \in \Omega^{Bus},\ t \in \Omega^T. \tag{47}$$

$$\underline{SOC} \leq SOC_{it} \leq \overline{SOC} \ : y_{23}^{it}, y_{24}^{it} \ \forall i \in \Omega^{Bus},\ t \in \Omega^T. \tag{48}$$

$$z_{it}^{c} + z_{it}^{d} \leq 1 \ \forall i \in \Omega^{Bus},\ t \in \Omega^T. \tag{49}$$

$$0 \leq P_t^{buy} \leq \overline{P^{buy}} \times ex_t^{in} \ : y_{25}^{t} \ \forall t \in \Omega^T. \tag{50}$$

$$0 \leq P_t^{sell} \leq \overline{P^{sell}} \times ex_t^{out} \ : y_{26}^{t} \ \forall t \in \Omega^T. \tag{51}$$

$$0 \leq Q_t^{buy} \leq \overline{Q^{buy}} \times ex_t^{in} \ : y_{27}^{t} \ \forall t \in \Omega^T. \tag{52}$$

$$0 \leq Q_t^{sell} \leq \overline{Q^{sell}} \times ex_t^{out} \ : y_{28}^{t} \ \forall t \in \Omega^T. \tag{53}$$

$$ex_t^{in} + ex_t^{out} \leq 1 \ \forall t \in \Omega^T. \tag{54}$$

$$0 \leq P_{it}^{DR} \leq P_{it}^{Int} \ : y_{29}^{it} \ \forall\ i \in \Omega^{Bus}, \forall t \in \Omega^T. \tag{55}$$

$$0 \leq P_{it}^{TDR} \leq H_{it}^{Int} \ : y_{30}^{it} \ \forall\ i \in \Omega^{Bus},\ \forall\ t \in \Omega^T. \tag{56}$$

3 | SOLUTION APPROACH

This section introduces the solution approach for addressing the robust resiliency formulation discussed earlier. The objective function and constraints of sample problem are presented in Equations (57)–(59), providing an overview of their general structure. In these equations, the matrix x represents the binary variables related to the commitment of CHPs, the commitment and location of MGs, and the binary variable indicating the reconfiguration structure of the distribution grid following a disastrous event. Furthermore, the matrix z comprises the operation variables, while the uncertain variables are denoted as $\emptyset$. The matrices c^T, b^T, F, f, A, B, g, and G contain the constant coefficients used within the formulation.

$$\min_{x} \left(c^T x + \max_{\emptyset} \min_{z} b^T z\right) \tag{57}$$

$$Fx \leq f \ binary \tag{58}$$

$$Ax + Bz \leq g - G\emptyset \ \forall z \in \Lambda(x, \emptyset) \tag{59}$$

The min-max-min sample objective function depicted in Equation (57) poses challenges for direct solution approaches. Here, a robust resiliency solution algorithm presented in Table 2 is proposed as an alternative. This algorithm leverages the C&CC algorithm and the strong duality theory to decompose and solve the problem [36, 37]. The objective function is divided into two optimization problems: the master problem and the sub-problem. The master problem, encompassing Equations (60)–(63), determines the optimal commitment of CHPs, optimal commitment and location of MGs, and optimal reconfiguration strategy. To facilitate the optimization process, a dual variable (y) is employed in these equations.

$$\min_{x,y} \left(c^T x + y\right) \tag{60}$$

$$y \geq b^T z_k \tag{61}$$

$$Fx \leq f \ x \ binary \tag{62}$$

$$Ax + Bz_k \leq g - G\emptyset_k^* \ \forall z \in \Lambda(x, \emptyset),\ \emptyset \in \varphi \tag{63}$$

TABLE 2 Robust resiliency solution algorithm.

C&CC Algorithm

1: Set $LB = -\infty$, $UB = +\infty$, $k = 0$ with determined initial $\emptyset_k^*$ and flag = no

2: While flag = no do

3: solve the master problem and obtain x^*, y^*

4: set $LB = c^T x + y^*$

5: solve the sub-problem and obtain z^*

6: Set $UB = c^T x^* + b^T z^*$

7: If $|UB - LB| \le \varepsilon$ then

8: flag = yes

9: end if

10: set k = k+1

11: add the $Ax + Bz_{k+1} \le g - G\emptyset_{k+1}^*$ and $y \ge b^T z_{k+1}$ constraints to the master problem

12: end while

13: Terminate the process

By utilizing a binary variable derived from the solution of the master problem, the optimal dispatch of CHPs, MGs, and ESSs can be determined. Furthermore, the optimal demand response program, optimal amount of load curtailment, and optimal procurement of electricity and thermal energy can be obtained by solving the sub-problem, as depicted in Equations (64) and (65). These calculations aim to minimize the total operation cost of CHPs, MGs, and ESSs, as well as the total customer interruption costs, gas costs, emission costs, costs associated with sold and purchased electricity, and demand response costs. It is important to note that these optimizations are conducted considering the worst-case scenario of stochastic data.

$$\max_{\emptyset} \min_{z} b^T z \tag{64}$$

$$Ax^* + Bz \le g - G\emptyset_{k+1} \ \forall z \in \Lambda(x, \emptyset), \ \emptyset_{k+1} \in \varphi \tag{65}$$

The sub-problem poses difficulties due to its max-min objective function, which cannot be easily solved using straightforward methods. To address this challenge, the sub-problem is transformed into a single-objective maximization problem by applying the strong duality theory. The resulting objective function is given as $\max_{y,\emptyset} y^T(g - G\emptyset - Ax^*)$ subject to $By^T \le b^T$, where y^T represents the matrix containing the dual variables. The dual objective function of this problem is outlined in Equations (66)–(87).

$$\begin{aligned}
\max_{y,\varphi} \Bigg[& \sum_{t\in\Omega^T} \sum_{i\in\Omega^{Bus}} \underline{P_i^{CHP}} \times u_{it}^{chp*} \times y_1^{it} \\
& + \sum_{t\in\Omega^T} \sum_{i\in\Omega^{Bus}} (PL_{li} - PL_{(l-1)i}) \times y_2^{it} + \\
& \sum_{t\in\Omega^T} \sum_{i\in\Omega^{Bus}} (P_{it}^{ED} - P_{it}^{W} - P_{it}^{PV}) \times y_3^{it} \\
& + \sum_{t\in\Omega^T} \sum_{i\in\Omega^{Bus}} Q_{it}^{ED} \times y_4^{it} + \\
& \sum_{t\in\Omega^T} \sum_{l\in\Omega^i} \beta_{lt}^* \times cap_l \times y_7^{it} - \beta_{lt}^* \times cap_l \times y_8^{it} \\
& + \sum_{t\in\Omega^T} \sum_{i\in\Omega^{Bus}} \overline{V} \times y_9^{it} + \underline{V} \times y_{10}^{it} + \\
& \sum_{t\in\Omega^T} \sum_{l\in\Omega^i} \overline{P}_i^{MG} \times u_i^{MG*} \times y_{12}^{it} - \overline{Q}_i^{MG} \times u_i^{MG*} \times y_{13}^{it} \\
& + \sum_{t\in\Omega^T} \sum_{i\in\Omega^{Bus}} P_{it}^{TD} \times y_{11}^{it} + \\
& \sum_{t\in\Omega^T} \sum_{l\in\Omega^i} \overline{P^{CHP}} \times u_{it}^{chp*} \times y_{14}^{it} - \underline{P^{CHP}} \times u_{it}^{chp*} \times y_{15}^{it} \\
& + \sum_{t\in\Omega^T} \sum_{l\in\Omega^i} \overline{Q^{CHP}} \times \\
& u_{it}^{chp*} \times y_{16}^{it} + \underline{Q^{CHP}} \times u_{it}^{chp*} \times y_{17}^{it} \\
& + \sum_{t\in\Omega^T} \sum_{l\in\Omega^i} \left(\left(2 - u_{i(t-1)}^{chp*} - u_{it}^{chp*} \right) \times \underline{P^{CHP}} + \right. \\
& \left. \left(1 + u_{i(t-1)}^{chp*} - u_{it}^{chp*} \right) \times RU^{CHP} \right) \\
& \times y_{18}^{it} + \left(\left(2 - u_{i(t-1)}^{chp*} - u_{it}^{chp*} \right) \times \underline{P^{CHP}} + \right. \\
& \left. \left(1 - u_{i(t-1)}^{chp*} + u_{it}^{chp*} \right) \times RD^{CHP} \right) \times y_{19}^{it} \\
& + \sum_{t\in\Omega^T} \sum_{l\in\Omega^i} \left(z_{it}^{c*} \times \underline{P^{BI}} - z_{it}^{d*} \times \overline{P^{BO}} \right) \times \\
& y_{21}^{it} + \left(z_{it}^{c*} \times \overline{P^{BI}} - z_{it}^{d*} \times \underline{P^{BO}} \right) \times y_{22}^{it} \\
& + \sum_{t\in\Omega^T} \sum_{l\in\Omega^i} \underline{SOC} \times y_{23}^{it} + \overline{SOC} \times y_{24}^{it} + \\
& \sum_{t\in\Omega^T} \sum_{l\in\Omega^i} \overline{P^{buy}} \times ex_t^{in*} \times y_{25}^{it} + \overline{P^{sell}} \times ex_t^{out*} \times y_{26}^{it} \\
& + \sum_{t\in\Omega^T} \sum_{l\in\Omega^i} P_{it}^{Int} \times y_{29}^{it} + \\
& H_{it}^{Int} \times y_{30}^{it} \Bigg]
\end{aligned} \tag{66}$$

In the dual objective function (66), non-linearity arises due to terms like $P_{it}^{ED} \times y_3^{it}$ involving $y^T G\emptyset$. Substituting Equation (1) with the dual objective function introduces non-linearity cases, represented by $ax = yv$, where ax, y, and v denote auxiliary, continuous, and binary variables, respectively. To handle this non-linearity, the problem is reformulated into a mixed-

integer linear formulation by employing the big-M approach for non-linearity terms, as demonstrated in Equations (67)–(70). Consequently, the maximum objective function is solved using methods based on MILP.

$$ax \le M \times v \tag{67}$$

$$ax \le y \tag{68}$$

$$ax \ge y - (1 - v) \times M \tag{69}$$

$$ax \ge 0 \tag{70}$$

Equations (71)–(91) outline the dual constraints in the problem. According to duality theory, the number of variables in the dual formulation matches the number of inequality equations in the original formulation. Likewise, the number of inequality equations in the dual formulation aligns with the number of variables in the original formulation. In the context of this problem, the associated original variables of the dual equations are explicitly identified as follows.

$$y_1^{it} - y_3^{it} - y_{11}^{it} \times \left(\frac{\eta_{th}}{\eta_e}\right) + y_{14}^{it} + y_{15}^{it} + y_{18}^{it} - y_{18}^{i(t-1)} + y_{19}^{i(t-1)} - y_{19}^{it} \le em^{chp} + G_{ref}^{CHP} \times \frac{\lambda_t^{gas}}{\eta_e} \ : P_{it}^{CHP} \quad \forall t \in \Omega^T, i \in \Omega^{Bus}. \tag{71}$$

$$-y_3^{it} + y_{20}^{it} - y_{21}^{it} + y_{22}^{it} \le \lambda_t \ : P_{it}^{ESS} \ \forall t \in \Omega^T, i \in \Omega^{Bus}. \tag{72}$$

$$-y_3^{it} + y_{27}^{it} \le \omega^{DR} \times \lambda_t \ : P_{it}^{DR} \ \forall t \in \Omega^T, i \in \Omega^{Bus}. \tag{73}$$

$$-y_3^{it} \le \rho_i^{EP} \ : P_{it}^{shed} \ \forall t \in \Omega^T, i \in \Omega^{Bus}. \tag{74}$$

$$-y_3^{it} + y_{12}^{it} \le 0 \ : P_{it}^{MG} \ \forall t \in \Omega^T, i \in \Omega^{Bus}. \tag{75}$$

$$y_3^{it} + y_{26}^{it} \le -\lambda_t \ : P_{it}^{sell} \ \forall t \in \Omega^T, i \in \Omega^{Bus}. \tag{76}$$

$$-y_3^{it} + y_{25}^{it} \le \lambda_t + em^{grid} \ : P_{it}^{buy} \ \forall t \in \Omega^T, i \in \Omega^{Bus}. \tag{77}$$

$$y_3^{it} + \frac{r_l}{V_1} \times y_5^{ijlt} + \frac{r_l}{V_1} \times y_6^{ijlt} + y_7^{lt} + y_8^{lt} \le 0 \ : P_{lt}^{f} \ \forall t \in \Omega^T, i \in \Omega^{Bus}. \tag{78}$$

$$-y_1^{it} + y_2^{llit} \le \alpha_{lli} \ : \gamma_{llit} \ \forall t \in \Omega^T, i \in \Omega^{Bus}, ll \in \Omega^{NL}. \tag{79}$$

$$-y_4^{it} + y_{16}^{it} + y_{17}^{it} \le 0 \ : Q_{it}^{CHP} \ \forall t \in \Omega^T, i \in \Omega^{Bus}. \tag{80}$$

$$-y_4^{it} \le 0 \ : Q_{it}^{DR} \ \forall t \in \Omega^T, i \in \Omega^{Bus}. \tag{81}$$

$$-y_4^{it} \le 0 \ : Q_{it}^{shed} \ \forall t \in \Omega^T, i \in \Omega^{Bus}. \tag{82}$$

$$-y_4^{it} + y_{12}^{it} \le 0 \ : Q_{it}^{MG} \ \forall t \in \Omega^T, i \in \Omega^{Bus}. \tag{83}$$

$$y_4^{it} + y_{28}^{it} \le 0 \ : Q_{it}^{sell} \ \forall t \in \Omega^T, i \in \Omega^{Bus}. \tag{84}$$

$$-y_4^{it} + y_{27}^{it} \le 0 \ : Q_{it}^{buy} \ \forall t \in \Omega^T, i \in \Omega^{Bus}. \tag{85}$$

$$y_4^{it} + \frac{x_l}{V_1} \times y_5^{ijlt} + \frac{x_l}{V_1} \times y_6^{ijlt} \le 0 \ : Q_{lt}^{f} \ \forall t \in \Omega^T, i \in \Omega^{Bus}. \tag{86}$$

$$y_5^{ijlt} - y_6^{ijlt} + y_9^{it} + y_{10}^{it} \le 0 \ : V_{it} \ \forall t \in \Omega^T, i \in \Omega^{Bus}. \tag{87}$$

$$-y_5^{ijlt} + y_6^{ijlt} + y_9^{it} + y_{10}^{it} \le 0 \ : V_{jt} \ \forall t \in \Omega^T, i \in \Omega^{Bus}. \tag{88}$$

$$E^{ESS} \times \eta_{\frac{ch}{dch}} \times \left(y_{20}^{it} - y_{20}^{i(t-1)}\right) + y_{23}^{it} + y_{24}^{it} \le 0 \ : SOC_{it} \ \forall t \in \Omega^T, i \in \Omega^{Bus}. \tag{89}$$

$$-y_{13}^{it} + y_{30}^{it} \le \omega^{TDR} \times \lambda_t \ : P_{it}^{TDR} \ \forall t \in \Omega^T, i \in \Omega^{Bus}. \tag{90}$$

$$-y_{11}^{it} \le \rho_i^{TP} \ : P_{it}^{Tshed} \ \forall t \in \Omega^T, i \in \Omega^{Bus}. \tag{91}$$

4 | CASE STUDY

To evaluate the effectiveness of the robust optimization approach in improving resiliency in the power distribution system, we focus on the modified IEEE 33-bus test distribution system. This system incorporates various components, including CHPs, ESSs, and RESs, as illustrated in Figure 2. Specifically, five CHPs are installed at buses 9, 12, 22, 25, and 29. Wind units (two) and PV units (five) are connected to specific buses (16, 19, 5, 7, 13, 21, and 27). ESSs (three) are assumed to be located at buses 8, 14, and 26. Detailed information about power demand, customer types, line data, and other relevant data can be found in [38]. The charge and discharge rates of the ESSs are limited to 250 kW per hour, with a charge efficiency of 0.85 and a discharge efficiency of 0.95 [39]. The initial state of charge (SOC) is set at 60%, and the acceptable SOC levels range from 0.2 to 0.9 [40]. Table 3 provides data on the CHPs, including their minimum power level, which is set at 5% of their nominal value. Load types are specified in [41], and the forecasted values for electrical active power load and thermal power load are depicted in Figure 3. Furthermore, the cost penalty associated with load interruptions for different customer types is considered, as referenced in [42]. The forecasted electricity prices are displayed in Figure 4 [43]. The active power output of wind and PV units is shown in Figure 5. The time horizon for the problem spans 24 hours. The acceptable voltage magnitudes range from $0.95^{p.u}$ to $1.05^{p.u}$ [44, 45]. From a computational perspective, the simulations were performed on a PC with an Intel Core i7 CPU @2.30 GHz and 8 GB RAM. The MIP master problem and sub-problem are modelled and simulated using GAMS software and the CPLEX solver.

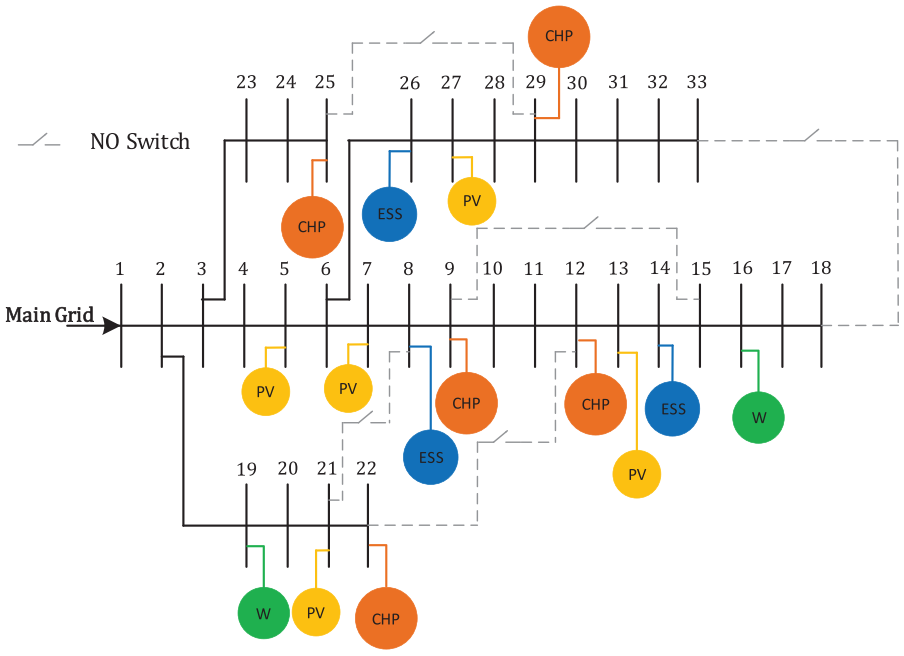

FIGURE 2 The modified IEEE 33-bus test distribution system.

TABLE 3 Specifications of the CHP units.

CHP #	Bus #	a	b	c	$\overline{P^{CHP}}$ (MW)	$\overline{Q^{CHP}}$ (MW)	c^{sp} ($)	c^{sd} ($)	RU^{CHP} (MW/h)	RD^{CHP} (MW/h)
CHP1	9	0	110	90	1	0.8	25	15	0.5	0.5
CHP2	12	0	110	90	1	0.8	25	15	0.5	0.5
CHP3	22	0	110	90	1	0.8	25	15	0.5	0.5
CHP4	25	0	110	90	1	0.8	25	15	0.5	0.5
CHP5	29	0	60	120	1.5	1.2	25	15	0.5	0.5

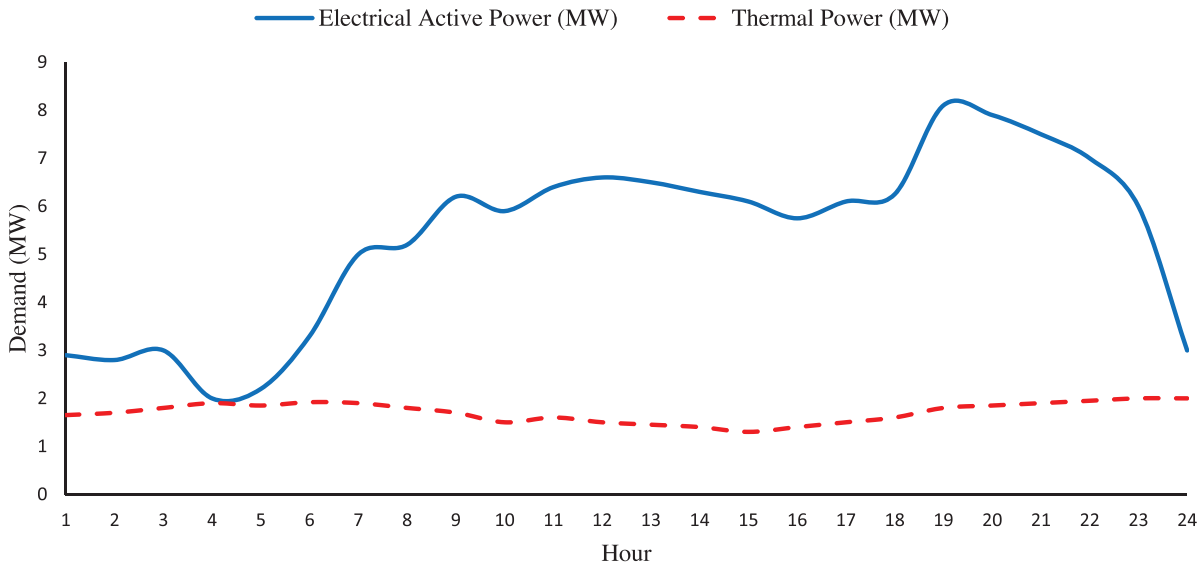

FIGURE 3 The forecasted value of electrical active power load and thermal power load.

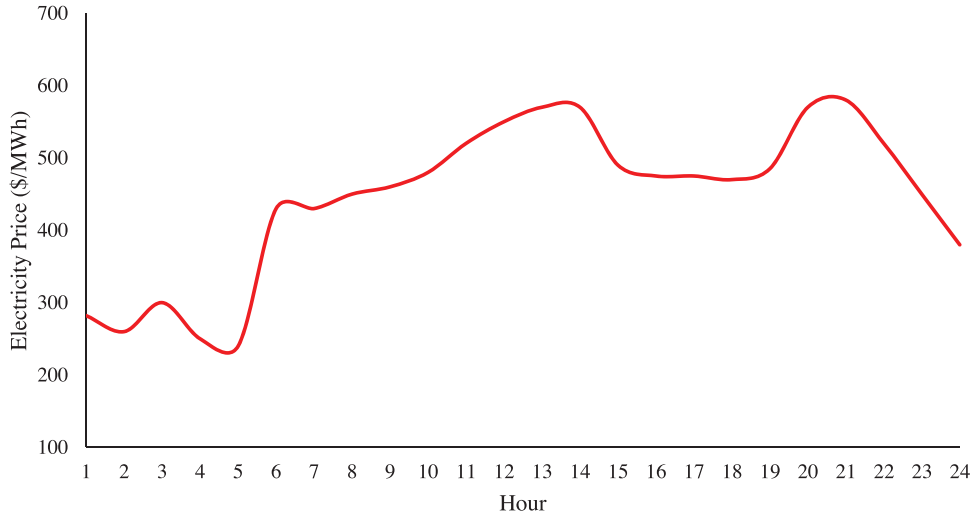

FIGURE 4 The forecasted value of the electricity price.

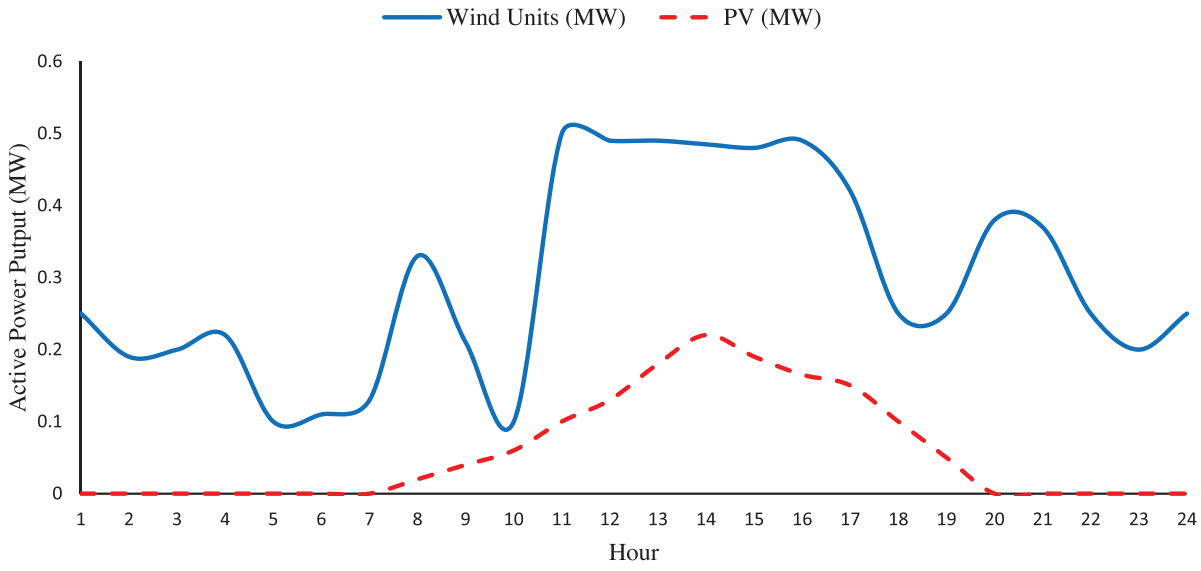

FIGURE 5 The active power output of wind and PV unit.

5 | RESULTS AND SENSITIVITY ANALYSIS

5.1 | Numerical results

In order to illustrate the fruitfulness of the aforementioned robust optimization approach for resiliency improvement in the power distribution system, four cases are considered in the test distribution system. These cases involve uncertain variables, including power load demand and price. The time Outage is supposed at 13 PM, consequently, lines 1–2, 2–19, 3–23, 4–5, 6–26, 10–11, 14–15, and 30–31 are damaged and they are out of service. The budgets of uncertainty for electrical loads and electrical prices are the same and considered as $\Gamma = \Gamma_P = \Gamma_\lambda = 24$. In addition, the errors in electrical loads and electrical prices are considered as $E_P = 7\%$ and $E_\lambda = 30\%$, respectively. In the first case "Case I", the outage occurred at hour 13 PM and then no resilient actions are performed. Thus, the robust resiliency formulation is solved for this case and the objective function (OF), TEC and $TCIC$ are equal to 535.596 k$, 21.45 k$, and 512.66 k$ as shown in Table 4, respectively. Moreover. The electrical and thermal supplied load also goes down to less than 55% and 52% as shown in Figures 6 and 7, respectively. In the second case "Case II", the outage occurred at 1:00 PM and then switching actions are performed to reduce the total cost and total interrupted load. Two crew teams are considered for this case and the time is needed for switching action with each team is equal to 1 h. the robust resiliency formulation is solved for this case and the objective function (OF), TEC and $TCIC$ are equal to 382.247 k$, 24.057

TABLE 4 Obtained results of all cases.

	OF (k$)	*TEC* (k$)	*TCIC* (k$)	*TCEM* (k$)	TC^{Grid} (k$)	TC^{Gas} (k$)	TC^{DR} (k$)	TC^{CHP} (k$)	TC^{ESS} (k$)
Case I	535.596	21.450	512.660	1.486	−4.862	7.455	0	18.372	0.485
Case II	382.247	24.057	356.608	1.582	−4.712	7.917	0	20.373	0.478
Case III	231.687	34.883	195.223	1.582	−4.686	7.917	10.801	20.373	0.477
Case IV	129.351	34.058	93.719	1.574	−4.683	7.876	9.578	20.798	0.489

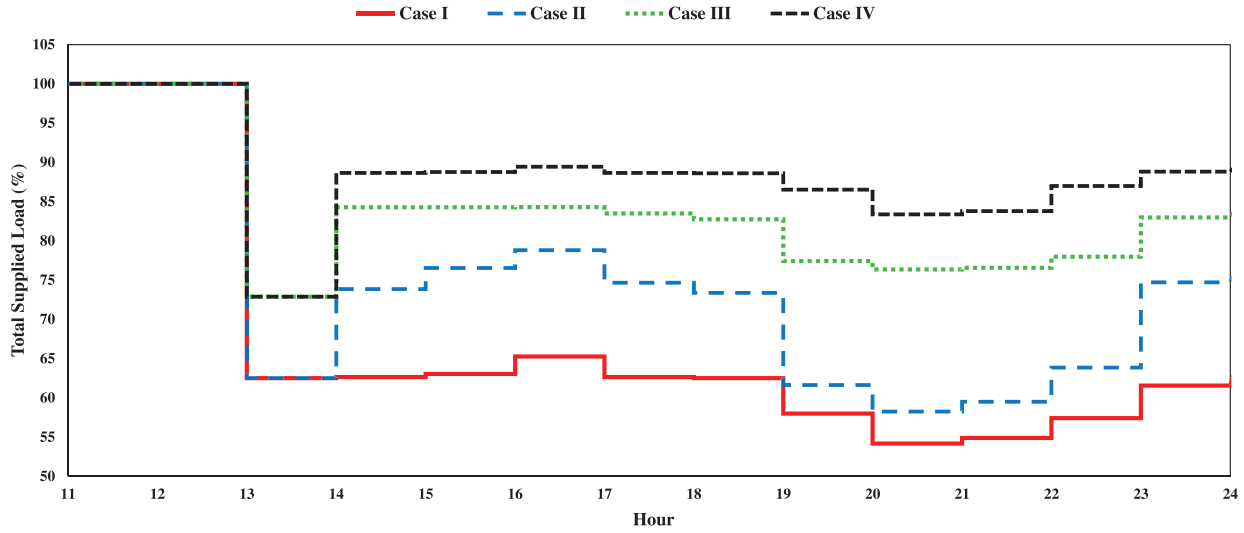

FIGURE 6 The results of the electrical supplied load.

k$, and 356.608 k$ as shown in Table 3, respectively. Moreover, the maximum and minimum supplied loads are about 80% and 60%, respectively, as depicted in Figure 6. The curtailment load decreases overall, indicating the efficacy of the robust optimization approach in handling uncertainty variables. Notably, the *OF* significantly decreases due to the closure of two normally open switches (9–15 and 25–29) by the two crew teams at 2:00 PM. This strategy leads to the formation of multiple microgrids and an increase in *TEC*, as depicted in Figure 8.

In the following, in third case "Case III", the outage occurred at 1:00 PM and then switching actions and demand response program are performed simultaneously to reduce the total cost and total interrupted load. As previously, 2 crew teams are considered for this case and the time needed for switching action with each team is equal to 1 h. The robust resiliency formulation is solved for this case and the *OF*, *TEC* and *TCIC* are equal to 231.687 k$, 34.883 k$, and 195.223 k$ as shown in Table 3, respectively. Moreover, the maximum and minimum electrical supplied loads are about 85% and 77% as shown in Figure 6, respectively, and it is shown the curtailment load is decreased overall compared to "Case I" and "Case II". As shown in the results, the *OF* are reduced significantly because two normally open (NO.) switches (9–15 and 25–29) are closed by two crew teams at 2:00 PM as well as performing a demand response program. In addition, by spending 10.801 k$ for performing the demand response program, *TCIC* is reduced by 161.385 k$. using this strategy, several microgrids are formed with the demand response program simultaneously and *TEC* is increased cause of the greater use of available resources and demand response program as shown in Figure 8. Furthermore, the percentage of demand response participation in "Case III" is displayed in Figure 9. As shown in this figure, the maximum and minimum participation of demand response program is about 16% of total load at peak hours and 4% at minimum load after the outage, respectively. Finally, in the fourth case "Case IV", the outage occurred at 1:00 PM and then switching actions and demand response program are performed simultaneously as well as using MGs to reduce the total cost and total interrupted load. As previously, 2 crew teams are considered for this case and the time needed for switching action with each team is equal to 1 h. Moreover, 2 MGs have existed in this case, and it is assumed that the time for transferring and utilization of each MG is equal to 1 hour. The robust resiliency formulation is solved for this case and the *OF*, *TEC* and *TCIC* are equal to 129.351 k$, 34.058 k$, and 93.719 k$ as shown in Table 3, respectively. Moreover, the maximum and minimum electrical supplied loads are about 90% and 85% as shown in Figure 6, respectively, and it is shown the curtailment load is decreased overall compared to "Case I", "Case II" and "Case III". As shown in the results, the *OF* are reduced significantly because two normally open (NO.) switches (9–15 and 25–29) are closed

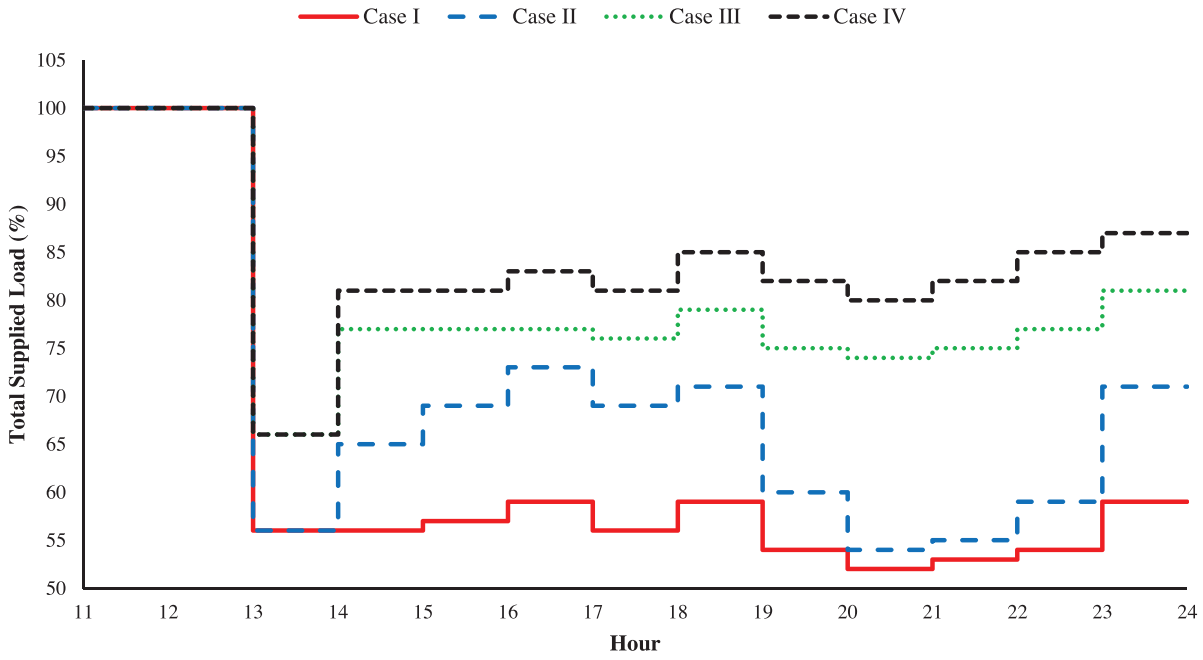

FIGURE 7 The results of thermal supplied load.

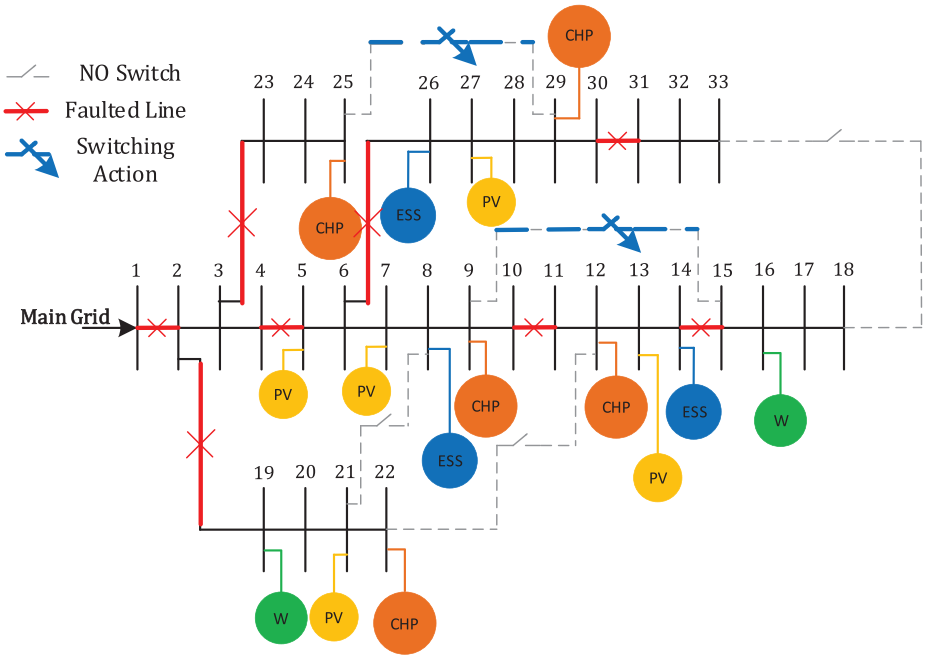

FIGURE 8 The IEEE 33 test system structure in "Case II" and "Case III".

by two crew teams at 2:00 PM as well as performing demand response program and utilization of two MGs in bus 3 and 17 at 2:00 PM, respectively. In addition, by spending 9.578 k$ for performing a demand response program and two MGs in this case simultaneously, *TCIC* is reduced by 101.504 k$. Using this strategy, several microgrids are formed with a demand response program and utilization of two MGs simultaneously, and *TEC* is decreased compared to "Case III" because of using MGs as shown in Figure 10. Furthermore, the percentage of demand response participation in "Case IV" is displayed in Figure 9. As shown in this figure, the maximum and minimum participation of demand response program is about 16% of total load at peak hours and 3% at minimum load after the outage, respectively. Moreover, the total participation of demand response is reduced compared to "Case III" cause of the utilization of MGs. As a consequence, the robust optimization approach, which

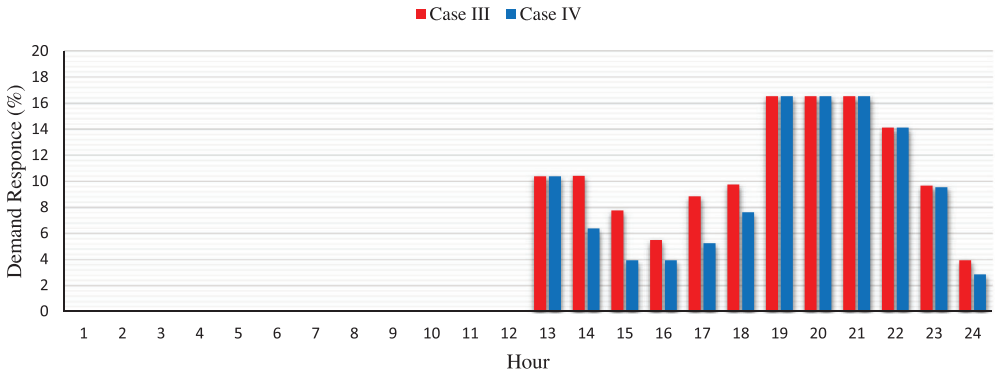

FIGURE 9 Percentage of demand response participation in "Case III" and "Case IV".

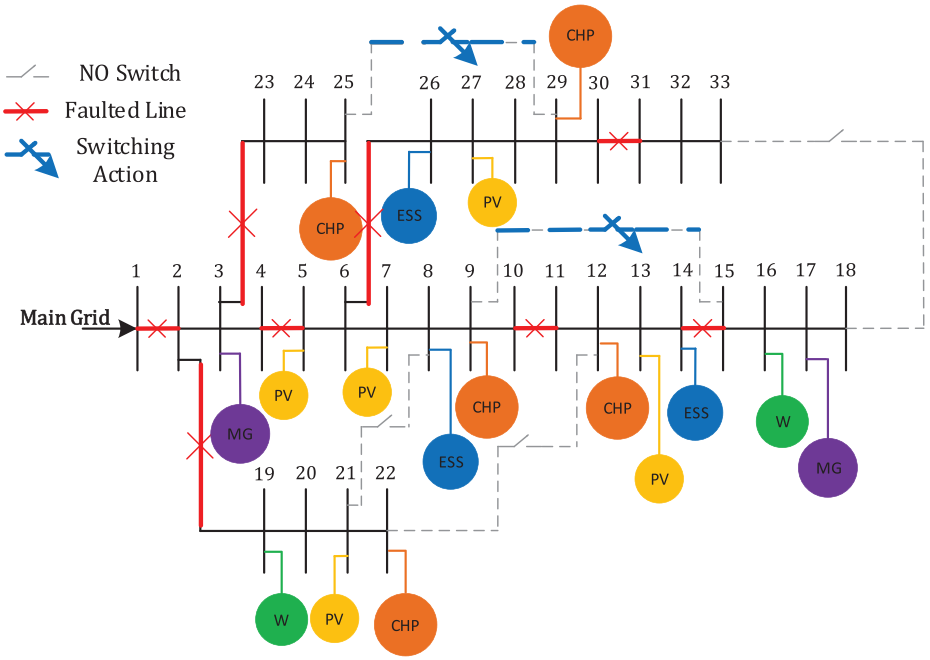

FIGURE 10 The IEEE 33 test system structure in "Case IV".

incorporates switching actions, demand response programs, and the utilization of MGs, has successfully reduced the total cost function and total curtailment loads. This approach effectively addresses the uncertainty associated with electricity load and price, leading to enhanced resiliency in the power distribution system.

While the effectiveness of the aforementioned approach has been previously demonstrated, it is important to consider various parameters that can influence the optimal solution for resiliency and total cost. Factors such as the budget of uncertainty and the number of crew teams for switching actions and MGs can significantly impact the outcomes. In order to evaluate the influence of these controllable parameters on the effectiveness of the proposed problem, a series of sensitivity analyses have been conducted.

5.2 | Sensitivity analysis of budget of uncertainty

In order to appraise the effect of budget uncertainty on the obtained results of the robust resiliency problem, a sensitivity analysis is performed in this part. For this purpose, the budget of uncertainty (Γ) is changed from 0 to 24 in 4 steps. For each budget of uncertainty, the robust resiliency approach in "Case IV" is solved and the obtained results are shown in Table 5. As expected, by increasing the budget of uncertainty, which is also called the degree of robustness, OF is increased. It means that increasing the budget of uncertainty leads to a more robust solution at the expense of higher robustness cost, such as the $TCIC$, TC^{DR} and TC^{CHP}. When the budget of uncertainty is equal to zero ($\Gamma = 0$), the robust problem is converted to the deterministic model with the OF equal

TABLE 5 Sensitivity analysis on budget of uncertainty in Case IV.

Γ	*OF* (k$)	*TCEC* (k$)	*TCIC* (k$)	*TCEM* (k$)	TC^{Grid} (k$)	TC^{Gas} (k$)	TC^{DR} (k$)	TC^{CHP} (k$)	TC^{ESS} (k$)
24	129.351	34.058	93.719	1.574	−4.683	7.876	9.578	20.798	0.489
20	128.470	33.703	93.257	1.510	−3.330	7.555	9.272	19.714	0.491
16	121.479	32.636	87.366	1.477	−2.543	7.390	8.111	19.171	0.507
12	117.717	32.051	84.214	1.452	−1.783	7.262	7.394	18.681	0.497
8	112.663	30.722	80.500	1.441	−2.149	7.241	6.535	18.608	0.487
4	110.673	29.920	79.326	1.427	−2.353	7.175	6.254	18.358	0.486
0	105.745	28.802	75.529	1.414	−2.748	7.132	5.808	18.220	0.389

TABLE 6 Sensitivity analysis on the number of crew teams for switching action.

Crew teams	*OF* (k$)	*TCEC* (k$)	*TCIC* (k$)	*TCEM* (k$)	TC^{Grid} (k$)	TC^{Gas} (k$)	TC^{DR} (k$)	TC^{CHP} (k$)	TC^{ESS} (k$)
2	231.687	34.883	195.223	1.582	-4.686	7.917	10.801	20.373	0.477
3	188.959	34.831	152.509	1.619	-4.704	8.108	9.949	20.969	0.508
4	162.268	37.182	123.444	1.642	-4.693	8.222	11.809	21.359	0.485
5	152.279	36.839	113.733	1.707	-4.534	8.532	10.063	22.282	0.496

to 105.745 k$. thus, the worst case has occurred in $\Gamma = 24$ and the total cost is not increased for the values above 24. Finally, this analysis shows the degree of robustness could be adjusted by using the budget of uncertainty (Γ) that which is considered the worst case for solving the model of this paper.

5.3 | Sensitivity analysis of the number of crew teams for switching action

In this part, a sensitivity analysis is applied to the number of crew teams for switching action in a robust resiliency approach. As mentioned before, each crew team is considered for one switching action, and the time for switching action is 1 h. The IEEE 33 bus test system in this paper has five normally open (NO.) switches, thus, the number of crew teams is changed from two crew teams to five crew teams and then the robust resiliency approach in "Case III" is solved and the results are obtained in Table 6. As shown in this table, by increasing the number of crew teams, the value of *OF* and *TCIC* are decreased and *TEC* increased until 4 crew teams and then decreased cause of changes in TC^{DR}. In addition, two NO. switches (9–15 and 25–29), three NO. switches (9–15, 25–29 and 8–21), four NO. switches (9–15, 25–29, 8–21 and 18–33) and five NO. switches (9–15, 25–29, 8–21, 18–33 and 12–22) are closed by two, three, four and five crew teams at 2:00 PM, respectively. Moreover, the maximum-minimum electrical and thermal supplied load for two, three, four, and five crew teams are about 85%–77%, 85%–77%, 93%–77%, 93%–86% and 80%–74%, 80%–76%, 87%–75%, 90%–84% as shown in Figures 11 and 12, respectively, and it is shown the curtailment load is decreased overall. Thus, this parameter is important for utilizing the microgrids in the restoration process in the resiliency approach.

5.4 | Sensitivity analysis of the number of MGs

In this section, a sensitivity analysis is applied to the number of utilizing MGs in a robust resiliency approach. As mentioned before, MGs have existed in this case and it is assumed that the time for transferring and utilization of each MG is equal to 1 h. For this purpose, the MGs are changed from 2 to 5 and the robust resiliency approach in "Case IV" is solved and the results are obtained in Table 7. As shown in this table, by increasing the number of MGs, the value of *OF*, *TCIC* and TC^{DR} are decreased and TC^{CHP} increased cause of utilization of the MGs. In addition, two, three, four, and five MGs, are utilized at the bus (3 and 17), (4, 15 and 33), (2, 3, 31 and 32), and (3, 4, 15, 31 and 33) at 2:00 PM, respectively. Moreover, NO. switches on buses 9–15 and 25–29 are closed when two MGs are performed and NO. switches on buses 18–33 and 25–29 are closed when three, four and five MGs are utilized. The number of MGs that are utilized in a robust resiliency approach must change the results of switching actions. As seen in the results, two isolated zones existed after occurrence without any energy resources including zone 1 (with bus numbers 2, 3 and 4) and zone 2 (with bus numbers 31, 32 and 33). At least one MG is located in zone 1 and when more than one MG is utilized, NO. switch in bus 18–33 are closed for interconnect zone 2 with another zone and at least one MG is located in Zone 2. Moreover,

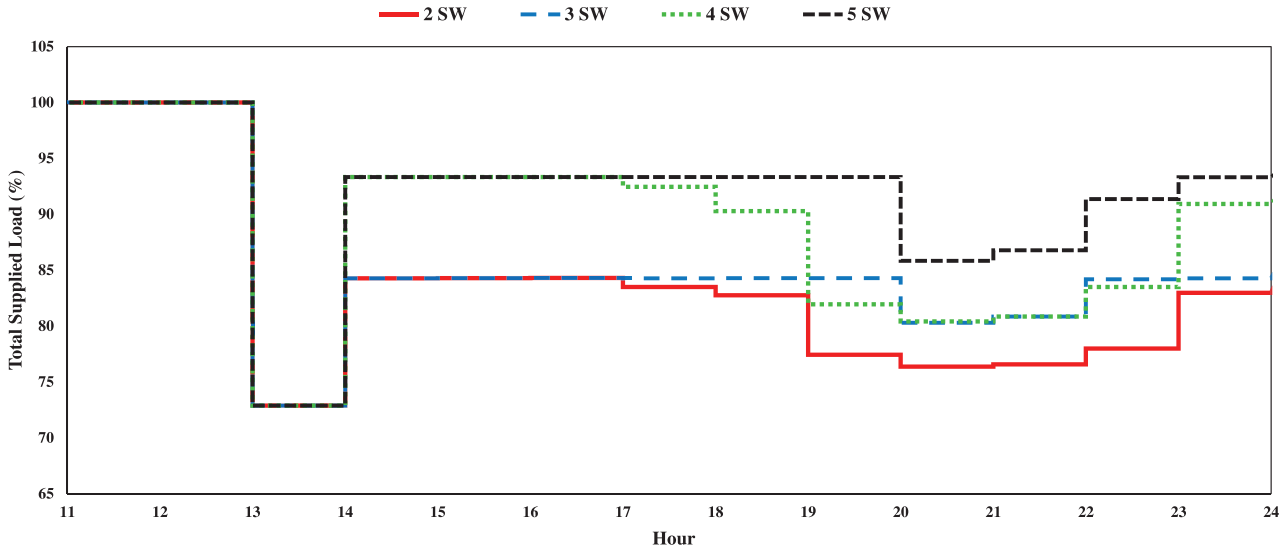

FIGURE 11 The results of the electrical supplied load for sensitivity analysis on the number of crew teams.

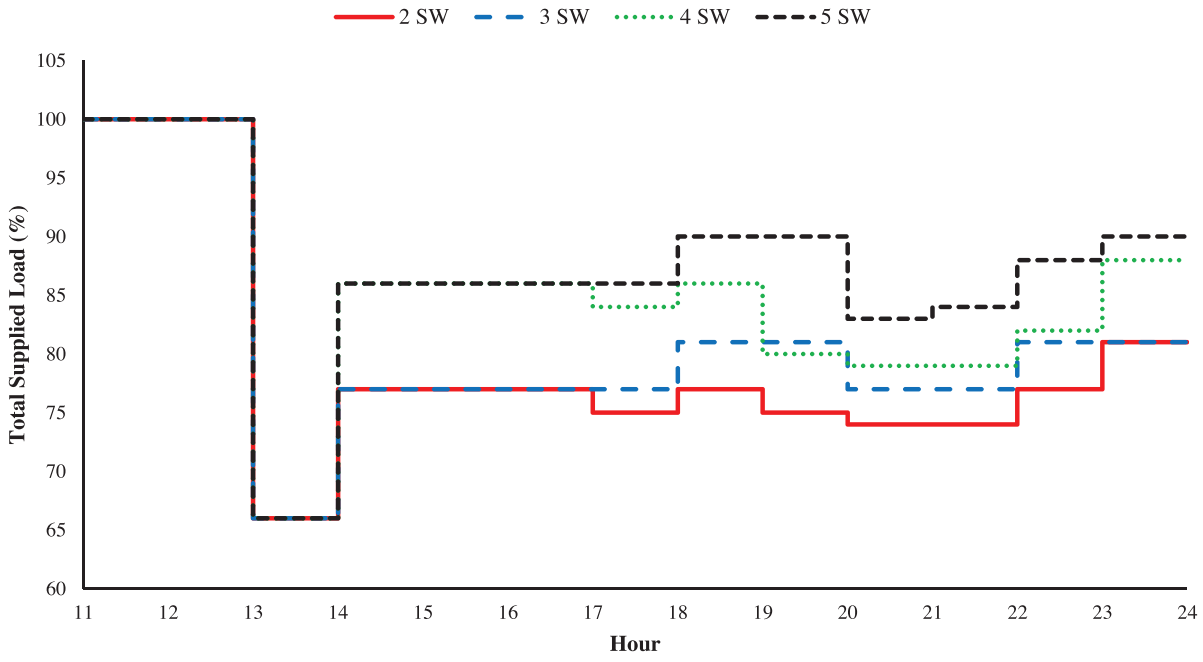

FIGURE 12 The results of thermal supplied load for sensitivity analysis on the number of crew teams.

TABLE 7 Sensitivity analysis on the number of MGs.

Number of MG	*OF* (k$)	*TCEC* (k$)	*TCIC* (k$)	*TCEM* (k$)	TC^{Grid} (k$)	TC^{Gas} (k$)	TC^{DR} (k$)	TC^{CHP} (k$)	TC^{ESS} (k$)
2	129.351	34.058	93.719	1.574	−4.683	7.876	9.578	20.798	0.489
3	93.201	34.366	57.270	1.565	−4.683	7.833	9.783	20.932	0.501
4	80.459	33.659	45.235	1.565	−4.704	7.833	8.841	21.168	0.522
5	70.629	33.808	35.256	1.565	−4.683	7.833	8.721	21.436	0.501

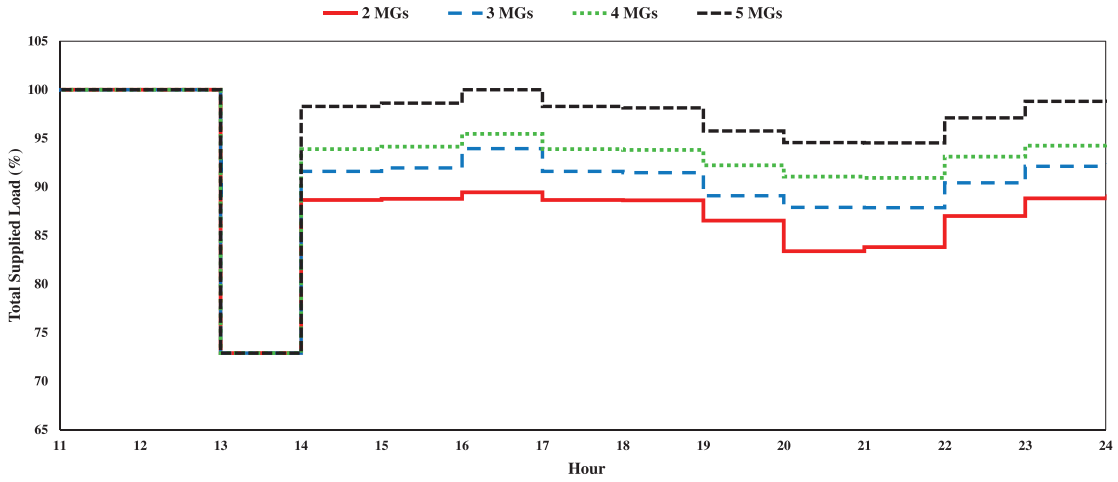

FIGURE 13 The results of the electrical supplied load for sensitivity analysis on the number of MGs.

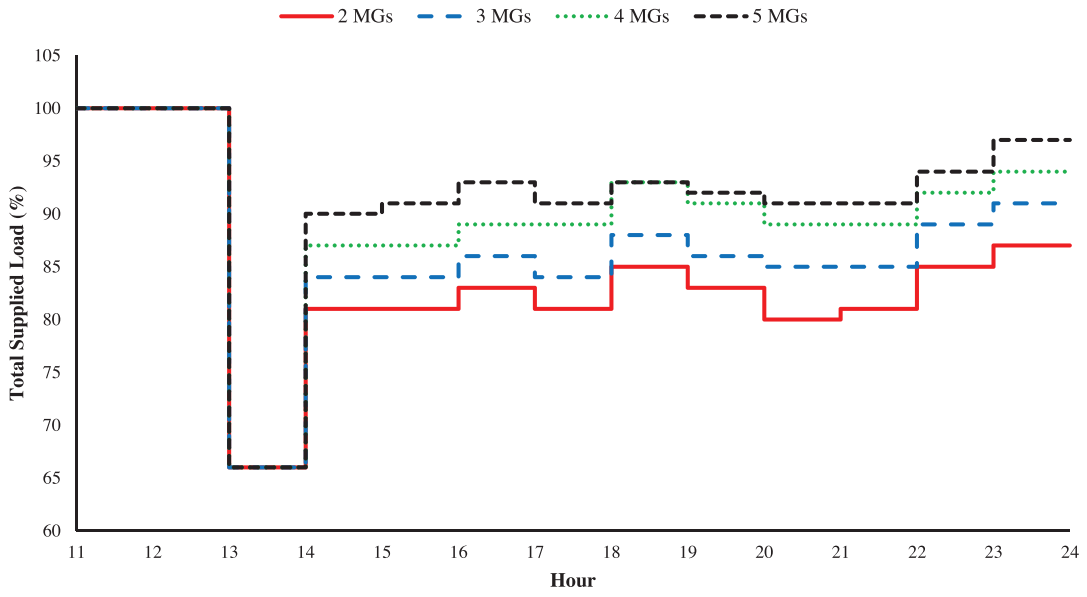

FIGURE 14 The results of thermal supplied load for sensitivity analysis on the number of MGs.

when five MGs are utilized, two of them are used in Zone 1, and another two are used in Zone 2 to reduce total cost and number of curtailed loads. In addition, the maximum-minimum electrical and thermal supplied load for two, three, four, and five MGs are about 90%–85%, 93%–88%, 95%–92%, 100%–95%, and 87%–81%, 89%–84%, 92%–87%, 96%–89% as shown in Figures 13 and 14, respectively, and it is shown the curtailment load is decreased overall.

5.5 | Sensitivity analysis of outage hour

In order to appraise the effect of outage hours on the obtained results of the robust resiliency problem, a sensitivity analysis is performed in this part. For this purpose, the outage hours are considered as 1:00 PM, 4:00 PM and 8:00 PM as a peak load. For each outage hour, the robust resiliency approach in "Case IV" is solved and the obtained results are shown in Table 8. As expected, increasing the load at 8:00 PM, *OF* in increased but the resiliency method worked properly. Also, the results at 4:00 PM show that the method can reduce the distribution system with a lower cost that presents an improvement in resiliency.

6 | CONCLUSION

The paper presents a robust optimization approach for enhancing the resiliency of power distribution systems. The objective function consists of minimum, maximum, and minimum functions, and the robust problem is solved using the C&CG method, which decomposes it into a master problem and subproblem. Uncertainty in electrical loads and electrical price is

TABLE 8 Sensitivity analysis on budget of uncertainty on case IV.

Hour	*OF* (k$)	*TCEC* (k$)	*TCIC* (k$)	*TCEM* (k$)	TC^{Grid} (k$)	TC^{Gas} (k$)	TC^{DR} (k$)	TC^{CHP} (k$)	TC^{ESS} (k$)
1:00 PM	129.351	34.058	93.719	1.574	−4.683	7.876	9.578	20.798	0.489
4:00 PM	118.11	32.373	84.239	1.498	−4.675	7.634	8.578	20.373	0.463
8:00 PM	165.848	40.735	123.521	1.592	−2.369	8.165	11.962	22.481	0.496

taken into account. The approach incorporates crew teams for switching actions, demand response programs, and MGs to improve system resiliency. Four study cases are defined to assess the effectiveness of the robust resiliency approach. The results demonstrate that the objective function of the robust formulation, considering switching actions, demand response programs, and MGs, achieves the lowest value compared to other cases. As quantitative research finding, the objective function (*OF*), and the total customer interruption costs (*TCIC*) are in "Case IV" as a final case, is decreased about 44.16%, 66.16% and 75.84%, and 51.99%, 73.71% and 81.71% from "Case III", "Case II" and "Case I", respectively. Notably, the robust method significantly reduces the total cost function and total curtailment loads by effectively handling the uncertainty of electricity load and price, thereby improving the resiliency of the power distribution system. A sensitivity analysis is conducted on the budget of uncertainty, revealing the adjustable degree of robustness through the manipulation of the budget. Increasing the budget of uncertainty leads to higher total costs compared to the deterministic model and identifies the worst-case scenario. Additionally, a sensitivity analysis on the number of crew teams and microgrids indicates that increasing these components results in a significant decrease in the total cost of the system, enabling the distribution system operator to determine the optimal number of tools for the resiliency process.

NOMENCLATURE

Sets

Ω^{Bus}	Set of the network bus.
Ω^{T}	Set of horizon time.
Ω^{l}	Set of lines.
$\Omega^{maneuver}$	Set of maneuver switches.
Ω^{NL}	Set of piecewise linear production cost.

Constants

$\lambda_t^{buy}/\lambda_t^{sell}$	The price for buying/selling the electricity from/to the main grid at time t.
λ_t^{gas}	Gas price in the t^{th} hour.
$\overline{V}/\underline{V}$	Maximum and minimum voltage.
$G_{ref}^{CHP}/G_{ref}^{AXB}$	The coefficient for consuming gas in CHP/auxiliary burner.
η_e/η_{axb}	Efficiently of the CHP/auxiliary burner.
ω^{DR}/ω^{TDR}	Price coefficient of electric/thermal demand response programs.
c^{sp}/c^{sd}	Cost of start-up/shut-down for CHP.
ρ_i^{EP}/ρ_i^{TP}	The cost should be paid to customers cause of interruption in electrical/thermal loads in bus i.
c_t^{em}	Emission penalty cost at time t.
$em^{grid/chp/axcb}$	Emission produced in main grid/CHP/auxiliary burner.
P_i^{ED}/P_i^{TD}	Electrical/thermal loads in the bus i.
$\overline{P^{CHP}}/\underline{P^{CHP}}$	Upper and lower limit of power of CHP.
RU^{CHP}/RD^{CHP}	Ram up/down of CHP.
η_{ch}/η_{dch}	Efficiency of Charge/Discharge of ESS.
E^{ESS}	Battery capacity of the ESS.
$\underline{P^{BI}}/\overline{P^{BO}}$	Limitation rates of charge/discharge for the ESS.
$\overline{SOC}/\underline{SOC}$	Maximum/minimum allowable SOC.
$\overline{P^{buy}}/\overline{P^{sell}}$	Maximum electricity can be bought from/sold to the main grid.
$P_{it}^{Int}/H_{it}^{Int}$	Interruptible electrical/thermal loads at time t in bus i.
$NCrew$	Number of crew teams.
NMG	Number of MGs.
$DistFlow$	Distribution load flow method
α_{lli}	The slope of block ll of the piecewise linear production cost function of unit i.

Functions

OF	Objective function.
TEC	Total energy cost.
$TCIC$	Total customer interruption costs.
$TCEM$	Total emission cost.
TC^{Grid}	Cost of power exchange with the main grid.
TC^{Gas}	Cost of gas consumed in the distribution grid.
TC^{DR}	Cost of demand response programs performed in the distribution system.
CP_{it}^{CHP}	Cost of the CHP unit in the bus i at time t.

Variables

P_t^{buy}/P_t^{sell}	The active power for buying/selling the electricity from/to main grid at time t.
v_{it}^{gas}	Gas consumed in system at time t in bus i.
P_{it}^{CHP}	CHP active power at time t in bus i.

H_{it}^{AXB} The heat of the auxiliary burner at time t in bus i.

P_{it}^{DR}/P_{it}^{TDR} The amount of electric/thermal demand response at time t in bus i.

$sui_{it}^{CHP}/sdi_{it}^{CHP}$ Binary variable for CHP started-up/shut-down at time t in bus i.

$P_{it}^{shed}/P_{it}^{Tshed}$ Electric/thermal shedding value at time t in bus i.

Em_t Total emission produced at time t.

y_n^{it} Dual variable.

P_{it}^{W}/P_{it}^{PV} Active production of wind and PV units in bus i.

u_{it}^{chp} Binary variable for CHP power at time t in bus i.

P_{it}^{ESS} Power injected by the ESS at time t in bus i.

z_{it}^{c}/z_{it}^{d} Binary variable for ESS charged/discharged at time t in bus i.

SOC_{it} State of charge of the ESS at time t in bus i.

ex_t^{in}/ex_t^{out} Binary variable for network electricity in/out to the main grid at time t.

V_{it} Voltage at time t in bus i.

δ_{ijt} Binary Variable equals 1 if bus j is the parent of bus i at time t.

β_{lt} Binary variable equals 1 if the switch of line l is closed at time t.

ϑ_{lt} Binary variable equals 1 if the switch condition of line l changes at time t.

u_i^{MG} The binary variable equals 1 if MG is dispatched in bus i.

γ_{llit} The power produced in block ll of the piecewise linear production cost function of unit i in period t.

AUTHOR CONTRIBUTIONS

Reza Abshirini: Writing—original draft; software; methodology; data curation. **Mojtaba Najafi**: Formal analysis; investigation; validation; conceptualization; writing—review and editing. **Naghi Moaddabi Pirkolachahi**: Formal analysis; investigation; validation; conceptualization; writing—review and editing.

CONFLICT OF INTEREST STATEMENT

The authors declare no conflicts of interest.

FUNDING INFORMATION

This research did not receive any specific grant from funding agencies in the public, commercial, or not-for-profit sectors.

DATA AVAILABILITY STATEMENT

All of the used data are available upon request from the corresponding author.

ORCID

Reza Abshirini https://orcid.org/0000-0001-5489-0916

REFERENCES

1. Gholami, A., Shekari, T., Amirioun, M.H., Aminifar, F., Amini, M.H., Sargolzaei, A.: Toward a consensus on the definition and taxonomy of power system resilience. IEEE Access 6, 32035–32053 (2018)
2. Panteli, M., Mancarella, P.: The grid: stronger bigger smarter? IEEE Power Energy Mag. 13(3), 58–66 (2015)
3. Chen, C., Wang, J., Ton, D.: Modernizing distribution system restoration to achieve grid resiliency against extreme weather events: an integrated solution. Proc. IEEE 105(7), 1267–1288 (2017)
4. Lei, S., Chen, C., Zhou, H., Hou, Y.: Routing and scheduling of mobile power sources for distribution system resilience enhancement. IEEE Trans. Smart Grid 10(5), 5650–5662 (2019)
5. Thakar, S., Vijay, A.S., Doolla, S.: System reconfiguration in microgrids. Sustainable Energy Grids Networks 17, 100191 (2019)
6. Ebrahimi, J., Abedini, M., Mahdi, M.: Optimal scheduling of distributed generations in microgrids for reducing system peak load based on load shifting. Sustainable Energy Grids Networks 23, 100368 (2020)
7. Hubble, A.H., Ustun, T.S.: Composition, placement, and economics of rural microgrids for ensuring sustainable development. Sustainable Energy Grids Networks 13, 1–18 (2018)
8. Hussain, A., Bui, V.H., Kim, H.M.: Microgrids as a resilience resource and strategies used by microgrids for enhancing resilience. Appl. Energy 240, 56–72 (2019)
9. Khodaei, A.: Provisional microgrid planning. IEEE Trans. Smart Grid 8(3), 1096–1104 (2017)
10. Farzin, H., Fotuhi-Firuzabad, M., Moeini-Aghtaie, M.: Enhancing power system resilience through hierarchical outage management in multimicrogrids. IEEE Trans. Smart Grid 7(6), 2869–2879 (2016)
11. Poudel, S., Dubey, A.: Critical load restoration using distributed energy resources for resilient power distribution system. IEEE Trans. Power Syst. 34(1), 52–63 (2019)
12. Lei, S., Wang, J., Chen, C., Hou, Y.: Mobile emergency generator prepositioning and real-time allocation for resilient response to natural disasters. IEEE Trans. Smart Grid 9(3), 2030–2041 (2018)
13. Che, L., Shahidehpour, M.: Adaptive formation of microgrids with mobile emergency resources for critical service restoration in extreme conditions. IEEE Trans. Power Syst. 34(1), 742–753 (2019)
14. Yao, S., Wang, P., Zhao, T.: Transportable energy storage for more resilient distribution systems with multiple microgrids. IEEE Trans. Smart Grid 10(3), 3331–3341 (2019)
15. Lei, S., Chen, C., Li, Y., Hou, Y.: Resilient disaster recovery logistics of distribution systems: Co-optimize service restoration with repair crew and mobile power source dispatch. IEEE Trans. Smart Grid 10(6), 6187–6202 (2019)
16. Xu, Y., Wang, Y., He, J., Su, M., Ni, P.: Resilience-oriented distribution system restoration considering mobile emergency resource dispatch in transportation system. IEEE Access 7, 73899–73912 (2019)
17. Kavousi-Fard, A., Wang, M., Su, W.: Stochastic resilient post-hurricane power system recovery based on mobile emergency resources and reconfigurable networked microgrids. IEEE Access 6, 72311–72326 (2018)
18. Bedoya, J.C., Xie, J., Wang, Y., Zhang, X., Liu, C.-C.: Resiliency of distribution systems incorporating asynchronous information for system restoration. IEEE Access 7, 101471–101482 (2019)
19. Sedgh, S.A., Doostizadeh, M., Aminifar, F., Shahidehpour, M.: Resilient-enhancing critical load restoration using mobile power sources with incomplete information. Sustainable Energy Grids Networks 26, 2352–4677 (2021)
20. Yao, S., Wang, P., Liu, X., Zhang, H., Zhao, T.: Rolling optimization of mobile energy storage fleets for resilient service restoration. IEEE Trans. Smart Grid 11(2), 1030–1043 (2019)
21. Bertsimas, D., Sim, M.: The price of robustness. Oper. Res. 52(1), 35e53 (2004)
22. Gilani, M.A., Dashti, R., Ghasemi, M., Amirioun, M.H., Shafie-khah, M.: Amicrogrid formation-based restoration model for resilient distribution systems using distributed energy resources and demand response programs. Sustainable Cities Soc. 83, 103975 (2022).

23. Nourollahi, R., Salyani, P., Zare, K., Mohammadi-Ivatloo, B.: Resiliency-oriented optimal scheduling of microgrids in the presence of demand response programs using a hybrid stochastic-robust optimization approach. Int. J. Elect. Power Energy Syst. 128, 106723 (2021)
24. Shi, Q., Li, F., Olama, M., Dong, J., Xue, Y., Starke, M., et al.: Post-extreme-event restoration using linear topological constraints and DER scheduling to enhance distribution system resilience. Int. J. Electr. Power Energy Syst. 131, 107029 (2021)
25. Zhu, J., Yuan, Y., Wang, W.: An exact microgrid formation model for load restoration in resilient distribution system. Int. J. Electr. Power Energy Syst. 116, 105568 (2020)
26. Biswas, S., Singh, M.K., Centeno, V.A.: Chance-constrained optimal distribution network partitioning to enhance power grid resilience. IEEE Access 9, 42169–42181 (2021)
27. Alizadeh, M., Jafari-Nokandi, M., Shahabi, M.: Resiliency-oriented islanding of distribution network in the presence of charging stations for electric vehicles. Int. Trans. Electr. Energy Syst. 30(12), E12670 (2020)
28. Gilani, M.A., Kazemi, A., Ghasemi, M.: Distribution system resilience enhancement by microgrid formation considering distributed energy resources. Energy 191, 116442 (2020)
29. Momen, H., Abessi, A., Jadid, S., Shafie-khah, M., Catalão, J.P.: Load restoration and energy management of a microgrid with distributed energy resources and electric vehicles participation under a two-stage stochastic framework. Int j. electr. power energy syst. 133, 107320 (2021)
30. Ghasemi, M., Kazemi, A., Bompard, E., Aminifar, F.: A two-stage resilience improvement planning for power distribution systems against hurricanes. Int. J. Electr. Power Energy Syst. 132, 107214 (2021)
31. Ghasemi, M., Kazemi, A., Mazza, A., Bompard, E.: A three-stage stochastic planning model for enhancing the resilience of distribution systems with microgrid formation strategy. IET Gener. Transm. Distrib. 15(13), 1908–1921 (2021)
32. Zhang, G., et al.: Mobile emergency generator planning in resilient distribution systems: a three-stage stochastic model with nonanticipativity constraints. IEEE Trans. Smart Grid 11, 4847–4859 (2020)
33. Bertsimas, D., Litvinov, E., Sun, X.A., Zhao, J., Zheng, T.: Adaptive robust optimization for the security constrained unit commitment problem. IEEE Trans. Power Syst. 28(1), 52–63 (2012)
34. Amjady, N., Dehghan, S., Attarha, A., Conejo, A.J.: Adaptive robust network constrained AC unit commitment. IEEE Trans. Power Syst. 32(1), 672–683 (2017)
35. Jabr, R.A., Singh, R., Pal, B.C.: Minimum loss network reconfiguration using mixed-integer convex programming. IEEE Trans. Power Syst. 27(2), 1106–1115 (2012)
36. Zeng, B., Zhao, L.: Solving two-stage robust optimization problems using a column-and-constraint generation method. Oper. Res. Lett. 41(5), 457–461 (2013)
37. Shahidehpour, M., Fu, Y.: Benders decomposition in restructured power systems. IEEE Techtorial, 383, 135441 (2005)
38. Baran, M.E., Wu, F.F.: Network reconfiguration in distribution systems for loss reduction and load balancing. IEEE Trans. Power Del. 4(2), 1401–1407 (1989)
39. Mohammadi Hosseininejad, S.M., Mirsaeedi, H., Heydari, S., Fereidunian, A., Lesani, H.: Self-healing enhancement through co-deployment of automatic switches and electric vehicle PLs in an electricity distribution network. IET Gener. Transm. Distrib. 14(17), 3508–3517 (2020)
40. Mirsaeedi, H., Fereidunian, A., Hosseininejad, S.M., et al.: Long-term maintenance scheduling and budgeting in electricity distribution systems equipped with automatic switches. IEEE Trans. Ind. Inf. 14(5), 1909–1919 (2018)
41. Bokhari, A., et al.: Experimental determination of the ZIP coefficients for modern residential, commercial, and industrial loads. IEEE Trans. Power Delivery 29(3), 1372–1381 (2014)
42. Mirsaeedi, H., Hassankashi, A., Sajjadi, M., Siano, P.: A mixed-integer linear programming approach to maintenance budgeting in electrical distribution networks considering repair time uncertainty. In: International Conference on Future Energy Solutions (FES2023), Vaasa, Finland (2023)
43. Abniki, H., Taghvaei, S.M., Mohammadi-Hosseininejad, S.M.: Optimal energy management of community microgrids: a risk-based multi-criteria approach. Int. Trans. Electr. Energy Syst. 28, e2641 (2018)
44. Hashemi, S.M., Fereidunian, A., Mirsaeedi, H., Lesani, H.: Optimal placement of normally open switches for distribution automation in smart grid. In: Smart Grid Conference (SGC). Dresden, Germany, pp. 1–6 (2017)
45. Sajjadi, M., Huang, K., Sun, K.: Participation factor-based adaptive model reduction for fast power system simulation. In: 2022 IEEE Power & Energy Society General Meeting (PESGM). Denver, CO (2022)

How to cite this article: Abshirini, R., Najafi, M., Pirkolachahi, N.M.: A robust optimization approach for resiliency improvement in power distribution system. IET Gener. Transm. Distrib. 18, 963–982 (2024). https://doi.org/10.1049/gtd2.13062